The Influence of different oxygen concentrations on GPR55 and MMP expression in the human placenta

eingereicht von Frederike Reischies
geb. 18.01.1987, Berlin

zur Erlangung des akademischen Grades : Doktorin der gesamten Heilkunde Dr. med. univ.

an der medizinischen Universität Graz

unter der Anleitung von
Priv. Doz. Mag. Dr. Martin Gauster

ausgeführt am
Institut für Zellbiologie, Histologie und Embryologie

Graz, 17.03.2014 .....
Frederike Reischies

Eidesstattliche Erklärung

ich erkläre eidesstattlich, dass ich die vorliegende Arbeit selbstständig verfasst habe, andere als die angegebenen Quellen nicht verwendet habe und die den Quellen wörtlich oder inhaltlich entnommenen Textstellen als solche kenntlich gemacht habe.

Graz, 17.03.2014 …….
Frederike Reischies

Danksagungen

Ich möchte mich zu allererst ganz herzlich bei meinem Diplomarbeitsbetreuer Herrn Priv. Doz. Dr. Martin Gauster bedanken, der mir mit viel Geduld und Freundlichkeit zur Seite stand.
Ich möchte mich außerdem bei Frau Dr. Gerit Moser und Frau Laura Mikorey für den Beistand im Labor bedanken.
Außerdem bedanke ich mich bei meinen Eltern.

Table of contents

Abstract

The G-protein coupled receptor (GPR)55 and its endogenous ligand lysophosphatidylinositol (LPI) has a modulating function on proliferation, differentiation and migration. These biological processes are important for the development of the human placenta. Matrix Metalloproteinases (MMPs) are enzymes capable of degrading the extracellular matrix, which is necessary for the implantation of the placenta into the uterine wall.

The aim of this study was to investigate the influence of LPI and different oxygen concentrations on the expression of MMPs 2,7,9,19 and GPR55 in the human placenta. First, trimester placenta explants were incubated under different oxygen (2.5%, 8%, 12% and 21%) concentrations, in presence or absence of LPI for 48 hours. RNA was then isolated and quantitative RT-PCR performed to analyse the gene expression of MMPs 2, 7, 9, 19 and GPR55.

Abstrakt (deutsch)

Der G-Protein gekoppelte Rezeptor GPR55 und sein natürlicher Ligand Lysophosphatidylinositol (LPI) spielen bei physiologischen Prozessen wie Proliferation, Differenzierung und Migration von Zellen eine wichtige Rolle. Diese Prozesse wiederum sind bei der Plazentaentwicklung während der Schwangerschaft von zentraler Bedeutung.

Matrix Metalloproteasen (MMPs) sind Enzyme, die in der Lage sind, die extrazelluläre Matrix zu spalten und sind bei der Implantation der Plazenta in die Uteruswand stark vertreten.

Ziel dieser Arbeit war es, den Einfluss von verschiedenen Sauerstoffkonzentrationen und von Lysophosphatidylinositol auf die Expression von GPR55 und MMP2,7,9 und 19 zu untersuchen.

Dafür wurden Plazenten des ersten Trimenons 48 Stunden in 2,5, 8, 12 und 21% Sauerstoff, mit und ohne LPI, inkubiert. Daraufhin wurde RNA aus dem Plazentagewebe isoliert und durch quantitative RT-PCR untersucht, um die Expression von GPR55 und den MMPs zu analysieren.

Introduction

Implantation and decidualisation

On the sixth day after conception, the blastocyste arrives in the uterine cavity and settles on the uterine wall for implantation. Implantation is only possible in a definite period of time, called "window of receptivity", when the uterine endometrium has transformed into a receptive environment. The endometrial stroma cells assimilate glycogen and lipids to provide histiotrophic supply for the growing embryo until the vascular gas exchange and nutrition supply in the placenta starts. These cells are called decidua cells and form the decidua, which is the term for the endometrium during a pregnancy. Hence, the uterine endometrium undergoes decidualisation under the influence of progesterone(1). Different from most animals, in humans the decidualisation takes place independent of the presence of a conceptus. After ovulation, progesterone is secreted from the corpus luteum during the midsecretory phase of the cycle, which leads to the remodelling of the uterine endometrium. The implantation of the blastocyst is an additional trigger, which enhances the histological changes in the decidua.

Elongated fibroblast like cells transform into Decidua stroma cells, they become enlarged round shaped cells with polyploid nuclei and contend a bigger amount of polyribosomes and rough endoplasmatic reticulum. These decidua stroma cells gain new cellular functions in order to influence the surrounding tissue, to assist the implantation. They start to produce and secrete laminin and fibronectin (new components of the extracellular matrix), matrix metalloproteinases and inhibitors of matrix metalloproteinases. They also synthesise hormones, cytokines, chemokines and peptides, such as insuline like growth factor binding protein, corticotrophin releasing hormone, prolactin, LIF, IL-8, GRO1, MIC-1, RANTES(2). The proliferation and decidualisation of the endometrial cells into decidua cells is regulated amongst others by a cytokine, LIF, belonging to the cytokine family IL-6. LIF is secreted by endometrial cells, which is stimulated by the influence of progesterone. Apart from LIF, several hormones and cytokines like IL-11, prolactin and preimplantation factor (PIF) are involved in the regulation. PIF leads to the upregulation of pro-adhesion molecules on the Decidua stroma cells, which promotes the implantation(3). Decidualisation and its synchrony with the development of the morula and blastocyst are crucial for successful implantation. This process is so complex that the approximate probability of conception is only 30%, half of which survive 20 weeks of gestation(2).

Syncytiotrophoblast

At the stage of implantation the blastocyst is built of the inner embryoblast cells and the outer trophoblast cells. The trophoblast cells, also called trophectoderm, form the extraembryonic membranes and the fetal part of the placenta. This outer layer of trophoblast cells differentiates further into two different cell layers, the underlying cytotrophoblast and the overlying multinucleated syncytiotrophoblast. The Syncytium (syncytiotrophoblast) is formed by proliferation, differentiation and membrane-membrane fusion with the underlying cytotrophoblast cells. Since the syncytium is mitotically inactive, its maintenance depends on continued proliferation and fusion of the subjacent cytotrophoblast layer.

It has been described in many studies that ageing or damaged nuclei in the syncytium are cumulated, forming syncytial knots, which are then shed into the maternal blood in the intervillous space. This hypothesis remains controversial but there is consensus that a high amount of trophoblast components is released into the maternal organism and can be detected in an even higher amount in complicated pregnancies. Some studies suggest that the shed syncytial knots support the suppression of the maternal immune response to antigens found in the syncytial knots by inducing peripheral tolerance. It is estimated that 100.000 - 150.000 syncytial knots are shed daily from the syncytium into the maternal blood (4).

The cell mass of the syncytiotrophoblast grows into the decidua and on the 9^{th} day after conception, lacunas starts to form in the syncytium.

These cavities fuse with each other to build the future intervillous space, leaving intervening pillars of trophoblasts, called trabeculae, from which the villous tree develops. While perfusion with maternal blood has not been established completely yet, these cavities are filled with maternal blood from ruptured capillaries and secretion from the uterine glands. This nutrient solution ensures sufficient histiotrophic supply for the embryo(5).

On the 12^{th} day after conception, the blastocyst is completely covered by the uterine epithelium, later on called decidua capsularis.

Extravillus trophoblasts and vessel transformation

First trimester cytotrophoblast cells are the "stem cells" of two possible differentiation pathways; they are located in the proximal cytotrophoblast cell columns of the anchoring villi. By spontaneous differentiation they can enter the villous pathway, wherein the cytotrophoblasts fuse with the syncytiotrophoblast or the invasive pathway, wherein the cells acquire invasive properties and emerge from the villi(6).

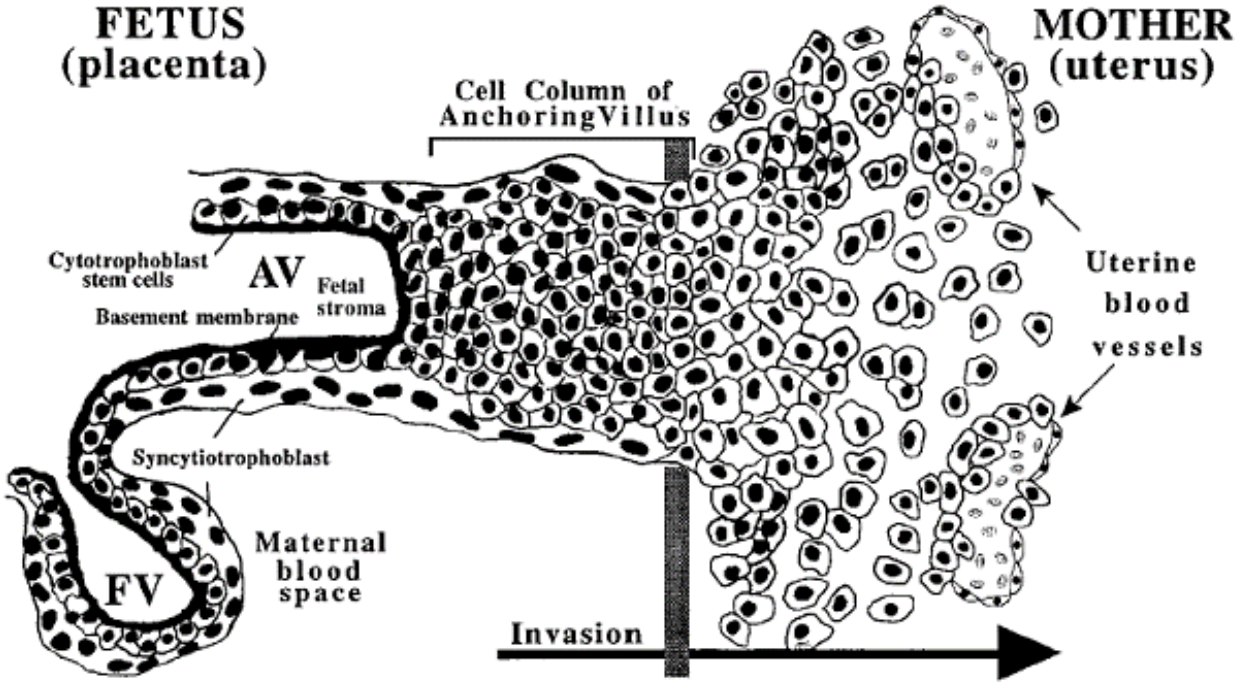

Figure 1, shows the invasion of the extravillous trophoblast cells into the uterine wall, where they target the uterine blood vessels. (Zhou et al., 1997)

By epithelial-mesenchymal transition the trophoblast cells start to form a new subpopulation, the highly proliferative villous cell collumn trophoblast. The high rate of proliferation within these cells is supposed to be maintained by the low oxygen concentration, which is physiological at this early stage of pregnancy and insulin-like growth factor-1/2.

To become extravillous trophoblast cells (EVTC), the villous cell column trophoblasts undergo growth arrest and emerge from the placental villi and migrate into the maternal decidua. Separated from the villi, the EVTC either modify the spiral arterioles or fuse with each other to form multinucleated giant cells, characteristic of the placental bed at term.

To transform the uterine vessels, the EVTC reach into the inner third of the myometrium, either moving through the interstitium or endovascular through the lumen of arterial vessels, specifically targeting the spiral arterioles.

Once the extravillous trophoblast cells have reached their target, they plug the spiral arteries. These plugs stop the maternal blood flow to the placenta and ensure low oxygen concentrations. For the first twelve weeks of pregnancy, during the organogenesis, the highly proliferating cells within the embryo need to be protected from oxygen concentration, which is physiological in the maternal blood.

However, at the end of the first trimester, the intra-arterial plugs are dissolved and the blood flow from the maternal organism to the placenta starts. At this stage of pregnancy, the growing foetus is no longer threatened by the oxygen concentrations in the maternal blood but needs a strong, steady blood supply from the uterine vessels, which begin to perfuse the intervillous space.

But the EVTC not only plug the spiral arteries, they also start a physiological process to transform these vessels. The transformation of the spiral arteries is induced by two different types of extravillous trophoblast cells. The endovascular trophoblasts induce apoptosis of the vascular smooth muscle and the endothelial cells. They then mimic an endothelial phenotype to replace the apoptotic part of the wall of the vessel, which leads to the transformation of spiral arteries into dilated rigid tubes, low in resistance, deprived of sympathetic innervation and unable to react to vasoconstrictive factors. These changes are supported by interstitial trophoblasts which induce vascular remodelling from outside (7). As a result of this transformation, the spiral arteries are no longer under control of the maternal organism, allowing a steady strong blood supply to the foetus.

This process of uterine vessel transformation is crucial for the health of foetus and mother. Many pregnancy-associated diseases are thought to be due to insufficient performance of the extravillous trophoblast cells, such as second trimester miscarriage, pre-eclamsia, pre-term birth and some forms of intrauterine growth restriction (8).

Villi

Before the maternal and foetal circulation start to exchange nutrients and metabolites, at ten weeks of gestation, the chorionic villous tree has to develop. The first placental villi start to develop at around day 13 post conception. Trophoblast trabeculae sprout finger-like outgrowths, which proliferate laterally into the intervillous space.

These first chorionic villi are growing all around the embryo but they perish where they are compressed by the decidua capsularis. Only in that area of the chorion where the placenta starts to form next to the decidua basalis are the villi able to develop and to branch out. The chorion with the atrophic villi is called the smooth chorion (*chorion leave*), the chorion which builds the placenta with the decidua basalis is called *chorion frondosum*. The formation of the chorion laeve is supported by the effect of the oxygen concentration in the maternal blood. In the area of the later chorion leave, the spiral arteries are not blocked by the extravillous trophoblast cells and are therefore perfused by maternal blood. In this area, connected to the maternal blood supply, the O2 concentration is relatively high in comparison to the very low oxygen concentration in the placental intervillous space at that time. By the influence of these relatively high oxygen concentrations, these villi undergo apoptosis and the chorion leave is formed.

Types of villi

The primary villus, which consists of only the cytotrophoblast surrounded by the syncythiotrophoblast, is the first villus type that appears at the surface of the trophoblast trabeculae.

Extraembrional mesenchyme, located between cytotrophoblast and embryoblast, starts to grow on the 15th day after conception into the trophoblast trabeculae. This extraembrional mesenchyme pushes the cytotrophoblast aside to the edge of the villi, forming the core of the secondary villus.

Finally, the tertiary villus develops when blood vessels appear in the central mesenchyme.

The vessels within the core of the tertiary villi do not sprout from the embryo through the umbilical cord into the placenta. They are formed by vasculargenesis, which is the term for vessel development in avascular tissue from differentiation of pluripotent mesenchymal progenitor cells.

Within the central mesenchyme of the tertiary villi, these first capillaries develop in the absence of pre-existing vessels, which starts at day 21 post conception (5). Angiogenesis describes the following connection of the preformed vessels with one another.

The tertiary villus is also called mesenchymal villus and differentiates from five weeks post conception further to form the mature villous tree (5).

First, the tertiary villi transform into immature intermediate villi (IIV), which are histologically characterised by a high subtrophoblastic density of capillaries due to branching angiogenesis within an expanded loose stroma. The loose stroma also contains matrix channels that provide a pathway for the Hofbauer cells, which are placental macrophages that patrol the villous core.

At the surface of the IIV trophoblast, proliferation leads to the outgrowth of sprouts, which in turn differentiate into mesenchymal villi.

At this stage, the new sprouting peripheral parts of the growing villous tree consist of mesenchymal villi, which transform into IIV at their bases. At the central parts of the villous tree, the IIV differentiate into stem villi. Stem villi are the foundation of the villous tree; in the mature placenta, 10 -16 generations of branching of stem villi can be found. The transformation of IIV into stem villi includes the regression of the peripheral capillary network, the reconversion of central capillaries into arterioles and venoles and the transformation of the villous core into dense stroma (9).

At 24 - 26 weeks of gestation, immature intermediate villi slowly vanish from the growing tree.

On the one hand, because they are constantly transformed into stem villi and on the other hand because their precursors, the mesenchymal villi or tertiary villi, start to produce mature intermediate villi.

Mature intermediate villi are deprived of core channels and contain long unbranched capillaries, which grow very quickly in longitudinal directions until capillary loops prolapse laterally into the wall of trophoblasts, forming terminal villi. Within the terminal villi, the capillaries are pushed to the wall of the villi and are thus very close to the intervillous space, forming the surface of gas exchange.

In the third trimester the formation of terminal villi increases exponentially, which is supported by non-branched angiogenesis in mature intermediate villi. The surface of gas exchange reaches 13m^2 by term(9).

Anchoring villi result from proliferation and ramification of stem villi that ultimately reach the basal plate. They are crucial for maintaining the placental inner structure and provide the origin for the development and proliferation of extravillous trophoblast cells.

The immensely huge surface of gas exchange is increased by microvilli located on the apical surface of the syncytiotrophoblast. These microvilli form an apical microvillous plasma membrane, which increases the villous surface to ensure sufficient gas- and nutrient exchange. They are supported by a network in the apical surface containing actin and microfilaments, which are adjacent to microtubules.

From the decidua basalis placenta septa grow towards the chorionic plate, they group one or two stem villi with all their branches together into 30 - 40 lobules, called cotyledones. Since the septa do not reach the chorionic plate, the blood can flow from one intervillous space into another, the barriers between the cotyledones are not closed.

Placental circulation

The maternal blood supply is completely established by the end of the first trimester of pregnancy. Through the spiral arteries, blood shoots pulsatile into the intervillous space, bathing the villi in blood. When the pressure decreases between pulses, the deoxygenated blood flows back into the uterine veins.

The deoxygenated blood, which is pumped by the foetal heard, reaches the placenta through the umbilical arteries. In the placenta, the umbilical arteries branch into chorionic arteries which branch further into cotyledon arteries. In the villi, a complex arterio-capillary-venous system is formed by these vessels. The capillaries bring the foetal blood closely to the maternal blood in the intervillous space, allowing the gas exchange. The oxygenated blood returns to the foetus through the umbilical vein.

The placental barrier

The placental barrier is the term for the tissue that separates the maternal from the foetal blood but allows the gas, nutrient and waste exchange. It is haemo-monochorial in term placenta and consists of the endothelium of the foetal vessel, the basal membrane, partly the cytotrophoblast and the syncytiotrophoblast with its microvilli. Towards the end of pregnancy the barrier becomes thinner (3,5µm), firstly because the foetal capillaries grow bigger and squeeze against the syncytiotrophoblast, pushing the stroma aside and secondly, due to exhaustion of cytotrophoblasts (10).

Active and passive transport mechanism through the placental barrier

Water and gas molecules such as oxygen and C02 can cross the membranes of the placental barrier by diffusion. Diffusion does not cost energy from ATP, but the molecules follow their concentration gradient. The molecules move from an area of high concentration to an area of lower concentration, which is driven by the entropy of the system. As long as the molecules are small enough, for example ammonia NH3, and urea CO(NH2)2 they can just pass through the membranes of the placental barrier.

The rate of passive transport for these small lipophilic permeants depends mostly on the blood flow, but the thickness of the barrier as well as its overall surface are important factors for the placental capacity for diffusional exchange (5).

In case of reduced blood flow in the uterine and also in the fetal department of the placenta, as it occurs in Intra uterine growth restriction (IUGR), the transfer rate of lipophilic solutes such as O2 and CO2 will decrease. But the reduced blood flow will have little effect on the transfer rates of hydrophilic solutes.

During the final trimenon, 20-30 ml oxygen crosses the placental barrier per minute(11)

Molecules that carry an electrical charge are not able to pass the placental barrier by diffusion. Since they are hydrophilic, they cannot pass through a hydrophobic area, such as the inner region of the phospholipid bilayer of a cell membrane. Their transfer is characterised as diffusion limited, which means they depend on barrier permeability.

For charged molecules, or molecules that are too big for diffusion, there are transmembrane

carrier proteins. The transport through these carrier proteins is called facilitated diffusion. Even though this way of transport depends on proteins, it does not cost energy. In case of water, the passive transport is called osmosis.

Any molecule that has to cross the membrane against its concentration gradient needs to be carried by active transport, which requires energy from ATPases. By active transport, it is possible to maintain significantly different serum concentrations of large molecules between the foetal and maternal organism. This transport way is mainly used from foetal to maternal direction for excretion of toxic metabolites and xenobiotics(12).

IgG, which crosses the placental barrier in foetal direction is transported by receptor mediated uptake, the receptor responsible is FcRn, the neonatal Fc immunoglobulin receptor. Maternal IgG molecules are actively transported into the foetal organism from the 14^{th} week of pregnancy, which is necessary for passive immunisation of the foetus.

Syncytial Membranes express cavedin and clathrin, molecules, which mediate endocytosis. Endocytosis is another active transport mechanism through the placental barrier for large polar molecules.

Amino acids are mainly actively transported over the placental barrier, since the amino acid concentration in foetal circulation is significantly higher than on the maternal side. An example for a transport system used by amino acids is the system A amino acid transporter family, which can be found on the membrane of the syncytium. Transporters belonging to this family carry small neutral amino acids such as glycine and serine over the membrane. This transport is sodium dependent, which means the transporters use the sodium gradient into the cell, which is maintained by Na+/K+ ATPase(5).

Glucose is very likely to be transported via transporter-mediated facilitated diffusion down its concentration gradient, since glucose concentrations are higher in maternal plasma. This transfer mechanism is independent of energy sources and sodium. Transporters in charge of glucose are members of the GLUT family, from which GLUT1 can be found highly expressed in term placenta (5). In early gestation, the foetal glycogenesis is very low; hence the demand for glucose is high. It increases throughout the pregnancy due to the rapid foetal growth, which significantly rises in the second trimester.

In pregnancy, the maternal serum lipids are elevated, which includes triglycerides, LDL cholesterol and apolipoprotein B. These increased levels support the transport through the placental barrier, which is highly regulated. In the trophoblast cells, lipids accumulate and are stored in lipid

droplets, which protects the foetal organism from too high lipid serum concentration and is used as a reservoir for energy and building blocks.

The placental barrier - drugs and medication

The placental barrier protects the unborn child from many nocent agents, nevertheless there are many substrates that can reach into the foetal organism and cause harm. In the 1960, the thalidomide scandal proved that the placental barrier is not impermeable to drugs taken by the mother. Today, drugs of small molecular weight <900kDA are thought to be able to cross from the maternal to the foetal organism. Most of the current medication dissolves into components of <900 kDA(5). These drug particles can cross the placental barrier by simple facilitated diffusion or by energy dependent mechanisms accomplished by transporter molecules.

Whether a drug can transfer the placental barrier and reach significant levels of concentration in the foetal organism depends on many factors. The placenta is able to accomplish extra-hepatic metabolism of drugs due to enzymes, located in the trophoblast, capable of biotransforming. These enzymes are similar to those in the maternal liver but may produce different metabolites, which can reach easily in to the foetal organism. CYP 3A4 biotransformes 50% of the common medications in the liver, but is not expressed in placental tissue. However, in the placenta CYP 19 metabolises many of CYP 3A4´s hepatic substrates. Nevertheless, drugs are different in their susceptibility to decomposition by these metabolic enzymes, depending on their physicochemical properties.

Apart from metabolic decomposition, drugs can be eliminated from the placenta by efflux transporters. For example methadone is a transport substrate of P-gp, P-glycoprotein efflux transporter, located in the placental apical membrane(5).

Substrate specificity for efflux transporters is not always an advantage. In antiretroviral therapy, placental transfer of the medication is desirable. Protease inhibitor drugs do not cross the placenta due to efflux transporters and can therefore not protect the foetus. However, Nucleoside reverse transcriptase inhibitors (NRVT) can cross the placental barrier unimpeded and reach therapeutic foetal blood concentrations. Thanks to these medication, perinatal transmission of HIV is <2%.

Apart from HIV, many virus types can cross the placental barrier, such as Rubella, Cocksackie, Parvovirus B19, Varicella - Zoster, etc. These viruses can cause generalised infection in the placental tissue, which results in decreased placental function and are associated with adverse pregnancy outcome.

Structure and function of the mature placenta

The human placenta separates and connects the mother and the foetus in order to prevent an immune rejection, but to allow the nutrients transfer and disposal of foetal wastes. At delivery the placenta has a disc shape and at measures in average 22cm in diameter and weights about 470g. The foetal and placental weights are directly proportional to each other(5).

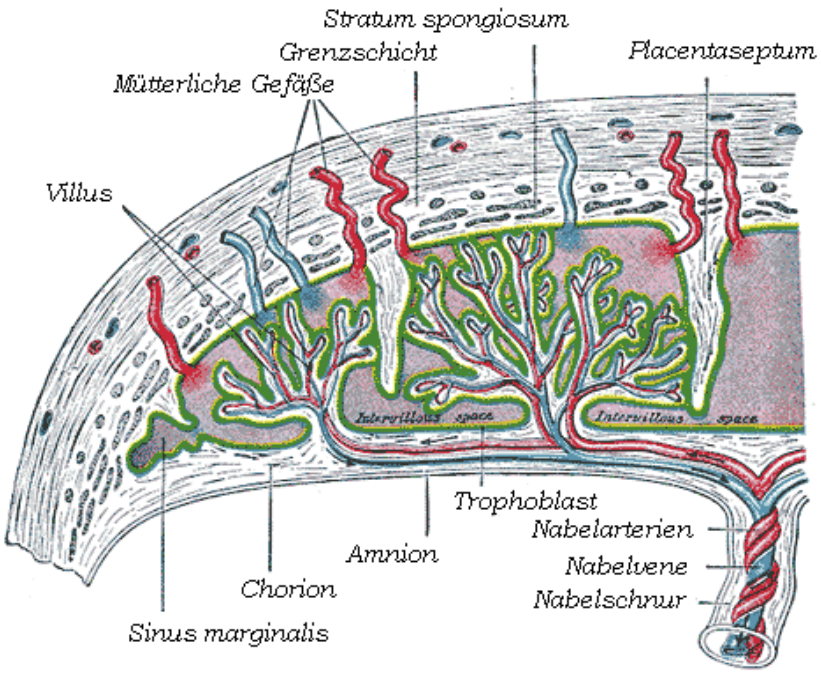

Figure 2, shows the structure of a human placenta, with maternal vessels, the villous tree and the intervillous space (from the 20th US edition of Gray´s Anatomy 1918)

The maternal part of the placenta consists of the decidua basalis in which the stem villi are anchored. On the surface of the decidua basalis the spiral arteries open into the intervillous space. The intervillous space is filled with 150 ml of blood.

The foetal part of the placenta consists of the chorionic plate, which carries the different types of villi. The Anchoring or stem villi, which are tightly connected to the decidua basalis hold the inner

structure of the placenta in place.

The surface of the placenta facing the foetus and the umbilical cord is covered with amnion. The amnion consists of a single layer of epithelium on a basement membrane. The amnion is attached to the chorion leave by an avascular connective tissue. The chorion leave is built of mesenchyme, mononuclear cytotrophobasts and vessels. The chorioamnion membrane houses the amniotic fluid.

The umbilical cord, containing two arteries and one vain, inserts into the chorionic plate and connects the foetus with the placenta, it measures about 50 - 60 cm at birth (10). The deoxygenated blood flows from the foetus to the placenta through the paired arteries, the oxygenated blood flows through the umbilical vain to reach the foetal organism. The two arteries are connected with each other by the Hyrtl´s anastomosis close to the insertion of the umbilical cord into the placenta.

The oxygenated blood in the foetal organism reaches the arterial circulation by the foramen ovale and the ductus arteriosus. A consequence of the anatomy of the foetoplacental umbilical circulation is that thromboemboli and inflammatory mediators from the placenta can directly enter the foetal arterial circulation and therefor the microcirculation of organs.

The surface of the umbilical cord is covered with an epithelium derived from the amnion, which consist of simple squamous cells. The vessels within the umbilical cord are surrounded by histological special connective tissue, called Wharton´s jelly. The gelatinous consistence of this extracellular matrix is due to its composition of mucopolysaccharides and is crucial to protect the umbilical vessels from compression. The umbilical cord develops from extraembryonic endoderm, in which the umbilical vessels develop independently from the vessels in the placenta and embryo. These vessels, which developed separately, will subsequently connect with each other.

In Wharton´s jelly pluripotent mesenchymal stem cells can be found, which can be collected and conserved after birth, since they may be useful for therapeutic applications later in live (5).

0_2 demand and supply

During the first trimenon, the intervillous O2 concentration is very low (15mmHg), partial pressure of oxygen, since at that time the intervillous space is free of maternal blood cells (5). This low O2 concentration is important to allow rapid cell division and it reduces the danger of DNA damage through free oxygen radicals during the foetal organogenesis.

The blood circulation and gas exchange between maternal and fetal blood starts at ten weeks of gestation, when the intra-arterial plugs, build by the extravillous trophoblast, are dissolved. At that stage of pregnancy, an exponential rise in foetal growth occurs, which increases the demand for energy, oxygen and nutrient supply. These demands can be met thanks to the transformed uterine vessels and the timely loss of the intra -arterial plugs. The intervillous oxygen concentration rises due to the sudden blood flow into the intervillous space from 15 to 60 mmHg. In the late second and third trimester, a gradual fall of the intervillous oxygen concentration has been measured. It is assumed that the increased extraction of oxygen by the foetus is responsible for the fall.

Oxidative stress

Researchers have suggested that the onset of maternal blood flow into the intervillous space is associated with oxidative stress for the placental tissue until the trophoblast cells can establish an adequate defence by increased expression of antioxidant enzymes, such as catalase, glutathione peroxidase and superoxide dismutase (SOD).

Within the synthyciotrophoblast, the mitochondria change from anaerobic to aerobic metabolism at the end of the first trimester. It has been suggested that the mitochondrial metabolism is impaired during the onset of maternal blood flow to the placenta and results in the generation of new mitochondria, which are equipped with greater antioxidant defence mechanisms, able to cope with the rising oxygen tension. Until the trophoblast has adapted to a higher oxygen concentration, an imbalance arises between increased generation of free radical species and the antioxidant defence, resulting in oxidative stress. Markers of oxidative stress, the expression of heat shock protein HSP70 and the formation of nitrotyrosine residues have been found in the syncytiotrophoblast during that time. This effect occurs in healthy pregnancies and is therefore likely to be a physiological state of temporary oxidative stress and the placental tissue recovers from possible harm from free oxygen radicals. Studies suggest that this state of physiological oxidative stress is useful in the stimulation of trophoblast differentiation from a proliferative to an

invasive phenotype, boosting the invasion of extravillous trophoblast cells (13).

However, if the antioxidative defence mechanisms are established too late or too weakly or if the rise in oxidative tension within the intervillous space arises too early in pregnancy, the oxidative stress causes great harm to the trophoblast, resulting in apoptosis.

Studies could show that dissolving of the plugs too early in gestation leads to a toxic high level of intervillous oxygen for the foetus and hence is associated with early pregnancy loss (13).

In approximately 2⁄3 of early pregnancy failures, reduced extravillous trophoblast invasion into the spiral arteries was found, which is associated with premature onset of maternal circulation into the intervillouse space(14). The contribution of oxidative stress to early pregnancy failure was supposed to be due to the loss of syncytial function, if the syncytium is damaged, beyond repair by free oxygen radicals.

Hypoxia

Hypoxia is defined as inadequate oxygen supply. Within the placenta it is important to differentiate three types of hypoxia, preplacental, uteroplacental and postplacental hypoxia. Preplacental hypoxia is caused by reduced oxygen content or tension within the maternal blood. Hence maternal hypoxemia or anaemia can lead to preplacental hypoxia. However, limitation of blood flow through the uterine spiral arteries towards the intervillous space leads to uteroplacental hypoxia, which is mainly caused by insufficient invasion of extravillous trophoblast cells. Finally, the foetoplacental circulation can be impaired, which leads to postplacental hypoxia, even though normally oxygenated blood reaches the intervillous space. True knots in the umbilical cord, velamentous cord insertion and dysplasia of the terminal villi can lead to impaired foetoplacental circulation.

Ischemia is caused when the blood flow ceases completely. Temporal ischemia of the placenta is commonly followed by ischemia-reperfusion, a resumption of normal blood flow. This event results in strong fluctuation of intervillous oxygen concentration and a decline in tissue oxygenation, which can lead to apoptosis, due to the lack of oxygen supply. However, the rapid reoxygenation during the ischemia-reperfusion can result in oxidative stress. Both effects are accompanied by tissue inflammation. Ischemia and its resulting fluctuations in oxygen supply have been made responsible, among others, by some researchers for the development of preeclampsia (5).

Impaired oxygen sensing or signalling of the trophoblast cells has been proposed to play a role in the maldevelopment of the villous tree and the insufficient invasion of the extravillous trophoblast cells, both factors of placental hypoxia. Impaired transformation of uterine spiral arteries leads not only to decreased blood flow, but also to an increased blood flow velocity, due to the narrow lumen of the arteries. The force of this blood flow into the intervillous space can damage the sprouts of the villous tree, which leads again to impaired foetoplacental circulation.
The appearance of abnormally high oxygen content within the intervillous space before the trophoblastic cells have established a sufficient antioxidant response, was also presented as a factor in some studies (5).

Hormone production of the placenta

The placenta fulfils a neuroendocrine function during pregnancy by producing many hormones that are similar to those produced by other organs, such as the hypothalamic or pituitary gland. However, the function of these hormones is different during the non-pregnant state.
The hormones and growth factors are produced by and secreted from the cytotrophoblast, the syncytiotrophoblast, villous stroma cells and Hofbauer cells.
Until the end of the 4th month, the corpus lutheum produces the progesterone that is needed to maintain the pregnancy. The corpus luteum itself is maintained by the production of human chorionic gonadotropin (hCG), which is produced by the placenta. The human chorionic gonadotropin is a glycoprotein, which is composed of two subunits from which the alpha subunit is identical with components of LH, FSH and TSH. The beta subunit is unique to hCG and can be detected by pregnancy tests, either as a dimer in maternal blood serum or as a degraded core fragment in the maternal urine.
Apart from its role as a stimulator of the corpus lutheum, the hCG seems to be involved in the relaxation of smooth muscles and uterine vessel dilatation, since hCG specific receptors have been found within the myometrium and around the vessels (5).
After the 8th week of gestation, the placenta produces enough progesterone, so that the corpus lutheum is dispensable. However, placental progesterone production depends on maternal cholesterol stores. Progesterone is crucial for the maintenance of uterine quiescence; lower levels of progesterone can lead to premature contractions. The maternal immune response to the foeto-placental allograft is also influenced by progesterone.

Additionally, the placenta produces Estriol. Placental estriol production is dependent on the precursor dehydroepiandrosterone-sulfate, which is produced by the foetal and maternal adrenal glands. Estriol induces growing of the uterus and of the mammary glands, and it influences the uterine blood flow, the progesterone production and the steroid metabolism.

The human chorionic somatomammotropin is similar to the human growth hormone from the anterior pituitary gland. This hormone affects the metabolism of the maternal organism during pregnancy to ensure sufficient energy supply for the foetus. It decreases maternal insulin sensitivity, which leads to higher blood glucose levels, on the same time it reduces the maternal glucose utilisation(11).

MMPs

Matrix Metalloproteinases are a large group of proteases. All MMPs have in common their ability to degrade the extracellular matrix proteins which surround every cell in the human organism.

The proteolytic function of the MMPs depends on a zinc atom(10), which is located in the catalytic domain of the enzyme. Apart from the active site that carries a zinc atom there are also active sites that help to connect the MMP with the extracellular matrix.

So far, there are 23 different types of MMPs known in the human organism (15).

The degrading of extracellular matrix is important in many physiologic processes such as, tissue repair, morphogenesis, differentiation, proliferation, apoptosis and angiogenesis (16). In pathological processes such as metastasis, cirrhosis and arthritis they are also involved (10).

Angiogenesis, the growing of new capillary, is an important factor in every physiological process that includes growing of new tissue. The ability of MMPs to degrade the extracellular matrix (ECM) is essential for angiogenesis. The MMPs create openings into the ECM which the new capillaries can grow into (17).

Since uncontrolled activation of MMP would be fatal for any living organism, the activation of MMPs is controlled by a complex system of inactive proenzymes and inhibitors. Many studies have described the central role that MMP molecules play in tumour growing and metastasis. Many cancer types are characterised as more aggressive and lethal when MMPs are overexpressed (17).

The inhibitors of the MMPs are called tissue inhibitor of metalloproteinases TIMPs (16). They are organised in a family, and include TIMPs1-4. The TIMP´s chelating group binds tightly to the zinc atom of the MMP´s active site.

Before the MMPs are ready to degrade proteins, they need to be activated. They are synthesised and secreted as inactive proenzymes. These MMPs proenzymes carry a cystein residue (18) that needs to be cleaved off in order to activate the MMP. This residue is connected to the zinc atom in the active site and prevents the connection of the MMP with a substrate (15). The activation by splicing the cystein residue is called cystein swich (18).

The MMPs are classified in different ways. Most commonly they are classified into four groups by their substrate and localisation: a) the collagenases, b) the gelatinases, c) the stromelysins and d) the membrane-type MMPs (15).

The collagenases contain all MMPs which are capable of triple-helical fibrillar collagenolysis, which is found in bones, dentin and cartilage. The MMPs 1, 8, and 13 belong to this group.

The gelatinases are MMP 2 and 9; they are capable of degrading collagen 4 and gelatin.

MMP 3, 10 and 11, belong to the stromelysins which are able to degrade extracellular matrix proteins other than the helical collagenes(15).

MMP 14, 15, 16, 17, 24, 25 are not secreted into the extracellular matrix but stay membrane associated.

A different option to classify the MMPs is by comparing their primary sequences, which suggests six sub-groups (A-F) but this way of evolutionary classification is not very common.

Both classifications are limited by new found MMPs that do not fit in any of them (15).

MMP2

MMP2, also known as gelatinase A is a 72 kDa type 4 collagenase.

MMP2 belongs to the group of gelatinases; it is able to degrade collagen type 4, which is a major component of basement membranes.

MMP2 is supposed to be a special member of the MMP group since it was found intracellular active, too. Intracellular MMP2 was shown to play a role in cardiac disease development (19).

The activation of the inactive proMMP2 molecule is accomplished by TIMP2. TIMP2 is normally an inhibitor of active MMPs but it was found to interact with proMMP2, which seems to be a new found activation mechanism (20).

MMP2 is expressed in extravillous trophoblast during the early stages of pregnancy. It is supposed to be the main gelatinase in week 6-8 of pregnancy (21).

MMP9

MMP9 and MMP2 are the two members of the gelatinases, which degrade collagen type 4. Like MMP2, MMP9 plays a key role in trophoblast invasion. It is expressed in extravillous trophoblasts and replaces MMP2 after the 6th week of pregnancy as the main gelatinase (20). MMP9 was found in elevated serum levels of women undergoing a missed abortion (21).

MMP7

MMP7, also called Matrilysin, is distinctively smaller than the other members of the MMP family, due to the lack of a C-terminal hemopexin domain(17).

MMP7 is secreted from its producing cell as promatrilysin which is inactive at 28kDa. Endoproteinases, plasmin and trypsin can activate promatrilysin by removing a 9kDa domain.

Matrilysin can degrade many components of the extracellular matrix such as fibronectin, type 4 collagen, elastin, vitronectin, aggrecan and proteoglycans.

Many studies have shown that matrilysin is overexpressed in many different types of cancer cells and is associated with a poor prognosis.

Since MMP7 is widely expressed in cancer cells many researchers have described its central role in tumour invasion. Its wide ability to degrade the extracellular matrix makes MMP7 an ideal peptidase which leads the way into the surrounding tissue of the primary cancer.

Matrilysin can also bring the healthy cells neighbouring the cancer into apoptosis (17).

MMP19

Due to some structural differences, MMP19 cannot be classified into one of the common groups for MMPs and was supposed to be the first found member of a new MMP sub-family (21). MMP19 carries a unique cystein in the catalytic domain, a C-terminal trail, an altered latency motif and a unique oligoglutamate insertion in the hinge region (22).

MMP19 can degrade many components of basement membranes such as collagen type 4, laminin and tenascin C. Due to this combination of substrates of MMP19 it is supposed to play a role in angiogenesis and vascular remodelling (23).

G protein coupled receptors

The G protein receptors are transmembrane proteins that cause signal transduction by activating enzymes which produce second messengers. These second messengers influence the metabolism of the target cell(24).

The G protein itself is found intracellular next to the transmembrane receptor. There are different types of G proteins, small G proteins, large heterotrimer G proteins and other G proteins. The most important type of G proteins are the heterotrimer G proteins (like GPR55). They are built of three subunits, alpha, beta and gamma. The alpha subunit is connected to GDP (guadindiphosphate), while inactivated. When the G protein coupled receptor changes its composition due to a binding ligand, the alpha subunit becomes connected to GTP and is therefore able to start the intracellular signalling pathway.
The G protein coupled receptor itself consists of seven hydrophobic helices, which are located in the double layer of the cell membrane. The N-Terminus is found extracellular, the C-Terminus intracellular, where the receptor is connected to the G protein.

When a molecule binds extracellular to the receptor it changes its composition and interacts with the alpha subunit of the G Protein and the GDP is exchanged for GTP. The alpha subunit now connected to GTP separates from the other subunits and moves towards the enzymes which are to be activated. These enzymes are able to produce second messengers which influence the metabolism of the cell.
This process is reactivated when, (after some time,) the alpha subunit hydrolyses the GTP to GDP and reconnects with the other subunits, so that the complete G protein is restored.
Since one G protein coupled receptor is connected to many G proteins, the effect of one ligand is boosted.
There are many enzymes that can be activated by the G Protein but the most important ones are adenylatcyclase and phospholipase C(24).

cAMP signal pathway

The second messenger produced by adenylatcyclase is cAMP. The adenylatcyclase removes two phosphate molecules from ATP to produce the cyclic molecule cAMP.
There are also inhibiting G proteins, which can repress the activity of adenylatcyclase and therefore lower the cAMP amount in the cell. To influence the metabolism of intercellular cAMP activates the protein kinase A.
The protein kinase A is built of four subunits - two regulatory and two catalytic subunits. The regulatory subunits have two binding sites for cAMP. When the cytosolic cAMP level rises, cAMP connects with the binding sites of the regulatory subunit and the two catalytic subunits are released.
The free catalytic subunits phosphorylate enzymes that influence the cell´s metabolism.
The protein kinase A can also influence the expression of genes.

The free catalytic subunits move into the cell nucleus and binds to CREB (cAMP response element binding protein). CREB is a transcription factor that connects to specific sequences of the DNA, called cAMP response elements. When CREB binds to these response elements, the expression of the downstream gene is alternated (increased or decreased)(24).

Phosphatidylinositol signal pathway

Phospholipase C is an enzyme which is also activated by the alpha subunit of G proteins. When activated it cleaves phosphatidylinositol 4,5-bisphosphate (PIP2) into inositol-1,4,5-trisphosphate (IP3) and diacyl glycerin (DAG).
The IP3 increases the intracellular Ca^{++} level. When IP3 connects to a receptor of the endoplasmic reticulum, which is connected to an ion channel, calcium streams from inside the endoplasmic reticulum into the cytosol(24).
The cytosolic calcium level rises from normal 10^-7 to 10^-5 mol/l.

GPR55

GPR55 is a G protein coupled receptor, which was introduced as a novel cannabinoid receptor CB3(25). GPR55 was first isolated and cloned in 1999. However, the classification of GPR55 has been difficult, since the receptor is phylogenetically distinct from the other two cannabinoid receptors CB1 and CB2(26). It shows low amino acid identity with CB1 and CB2 and does not express the classical cannabinoid binding pocket. To understand the GPR55 binding pocket, models of GPR55 in its active and inactive state were constructed. In the active conformation of GPR55, important amino acid interactions during ligand binding where analysed. These models showed a highly hydrated binding pocket, which consists of many hydrophilic residues, whereas the binding region of the CB1 and CB2 are highly hydrophobic (27).

The third extracellular loop of GPR55 is the longest and consists of many charged amino acids. It is longer than the third extracellular loop of CB1 and CB2 and due to its charge it is supposed to be solvated in water. The 6th and 7th transmembrane regions of GPR55 are connected by this charged extracellular loop. Molecular dynamic simulations and covalent labelling studies suggest an entry pathway for lipid ligands with large head groups like LPI in-between these transmembrane regions 6 and 7 (28).

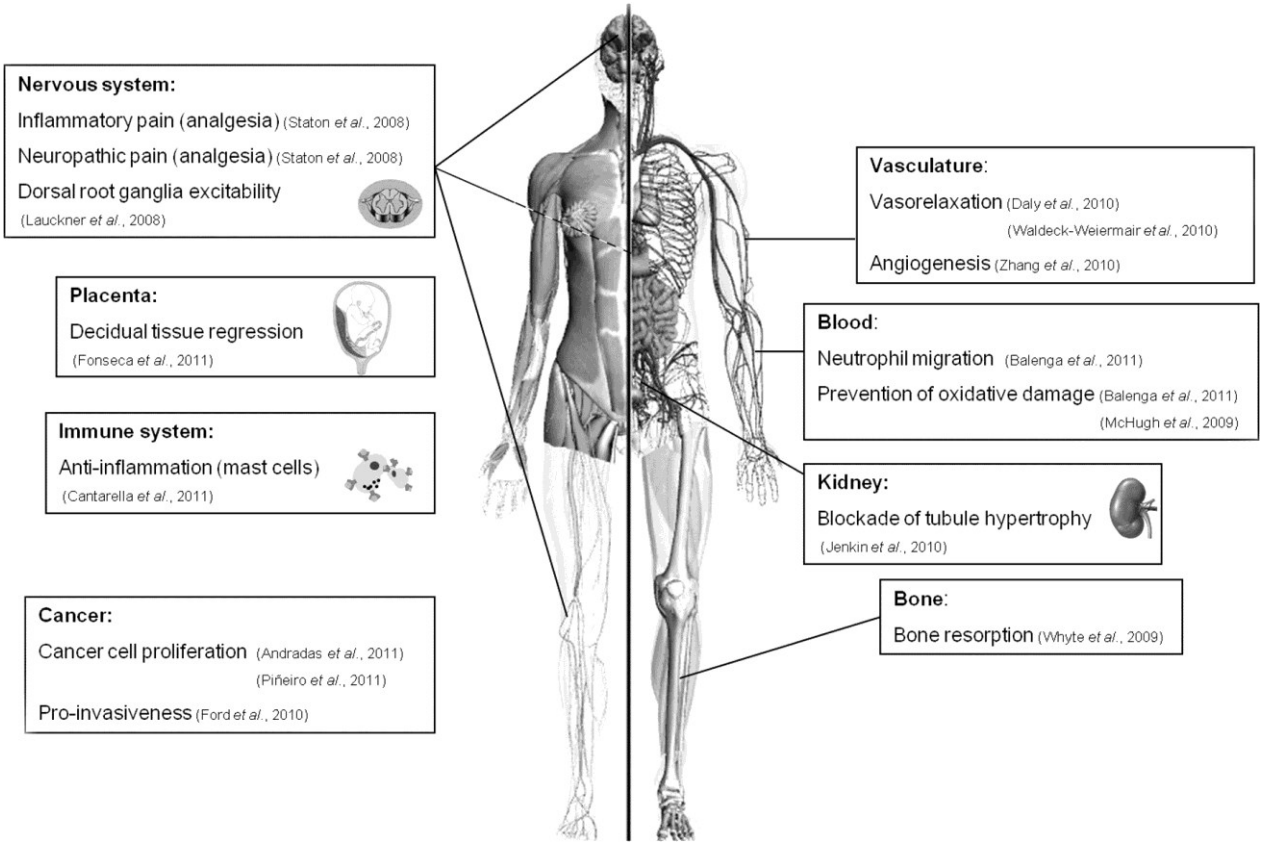

Figure 3, shows physiological and pathological systems and processes in which GPR55 is involved (from Henstridge, C M et al. Molecular Endocrinology 2011; 25:1835-1848)

Although several cannabinoid ligands can bind GPR55 its most consistent agonist is the non-cannabinoid endogenous lipid, lysophosphatidylinositol. In many studies, the cannabinoid ligands for GPR55 were described with significant inconsistency as agonists, antagonists or to have no effect at all.

The intracellular sorting of GPR55 was studied mostly in recombinant cell systems. After prolonged agonist stimulation GPR55 was down regulated after internalisation by targeted degradation. In the degradation process of GPR55 the GASP-1 was found to play an important role. GASP-1 is a G-protein coupled receptor associated sorting protein. In cells where GASP-1 was not present, GPR55 moved back to the cell surface after internalisation, avoiding intracellular enzymatic degradation and removal (28).

GPR55 was detected in rat decidua tissue. During the process of dezidualisation and placental development, the endocannabinoid system and therefore also GPR55 was proposed to regulate the metaplasia and apoptosis of former endometrial stroma cells. This is necessary to accommodate the growing embryo. In rodents GPR55 seems to play a central role in the regulation of uterine remodelling during pregnancy. Higher levels for GPR55 where found at that time of pregnancy where decidual regression was very important for placental growth, indicating a link between GPR55 levels and the uterine remodelling process (29).
Since in this study GPR55 was also found in uterine natural killer cells, it is suggested that GPR55 is required for the maintenance of pregnancy. It was also indicated that GPR55 stands in relation with the relaxation of the muscles of the pregnant uterus, which is crucial until labour.
In other studies, a vasodilatory effect mediated by GPR55 was already described, so it was suggested, that GPR55 assist in the remodelling process of the spiral arteries during pregnancy.
The expression pattern of GPR55 in decidua and uterine natural killer cells proposes that a disruption in the system of GPR55 and its ligands may cause problems in decidua regression, proliferation and differentiation (29).

Apart from the uterine tissue GPR55 is also expressed in many other tissues.
For example mRNA expression data confirms that GPR55 is also expressed in neutrophils. Studies have shown that LPI is an agonist for GRP55 in neutrophils, which leads to Rho-A dependent chemotaxis. The authors suggest that the chemotaxis to reach inflammatory loci is enhanced by the GPR55 system. Also LPI levels are higher in inflammatory tissues where it is secreted by macrophages (30).

In bone tissue, GPR55 seems to play a role in the regulation of bone metabolism. GPR55 was found both in osteoclasts and osteoblasts cells. The function of GPR55 in osteoblast remains unclear, however in osteoclasts GPR55 activation results in osteoclastogenesis and bone resorption.
This study has also shown that male GPR55 knockout mice show osteoporotic bone structures (31).

GPR55 is also widely expressed in human tumour cells, such as breast, ovary, and cervix, prostate, skin and liver. Studies could show that GPR55 levels even correlate with the aggressiveness of the tumour. The mRNA levels of GPR55 where higher in tumours expressing a histological unfavourable grade, compared with non-aggressive (low grade) tumours and healthy tissue. In glioma patients elevated mRNA GPR55 levels even correlated with decreased overall survival. These studies

suggest that GPR55 enhances the oncogenic capability of cancer cells. A higher proliferative capability in tumour cells which show overexpression of GPR55 has been proved, whereas genetic blockade of GPR55 has resulted in depression of the proliferation rate in tumour cell lines (32).

Apart from the elevated proliferative rate GPR55 seems to also increase the metastatic potential of tumour cells. A study has shown that a highly metastatic breast cancer cell line expresses 30 times higher levels of GPR55 than a comparable breast cancer cell line which is classified as low metastatic. This could indicate a relation between the metastatic potential and the expression rate of GPR55. It has also been reported that breast cancer cells artificially overexpressing GPR55 increase their migration towards chemoattractants, whereas cells with lower rate of GPR55 expression did not migrate towards specific serum factors. In this study, higher LPI levels could additionally enhance the migration of the breast cancer cells (33).

LPI, the ligand of GPR55

Lysophosphatidylinositol belongs to the group of lysophospholipids. They are products of the enzyme phospholipase A, which hydrolyses membrane phospholipids into lysophospholipids and free fatty acids. Since Lysophospholipids are also components of the plasma membrane, it was assumed that they modulate the membrane structure by changing the mechanical properties of the bilayers. But research data suggested that Lysophospholipids also play a role as signalling molecules (34).

In all research data Lysophosphadidylinositol is characterised as the most potent and consistent agonist for GPR55. The role of this phospholipid was until the mid-80s not well understood. It was found that LPI could stimulate the release of insulin from pancreatic islets(34). Then some studies could show that oncogenic transformed cell lines accumulated LPI. Due to the accumulation of LPI as a consequence of malignant cell transformation, it was now assumed to be involved in the regulation of cell proliferation (35). Even though LPI was identified as a potent mitogenic factor its signalling pathway was not understood. Research data suggested the existence of a specific receptor for LPI on the cell membrane (36). In 2007, GPR55 was finally identified as a specific receptor for LPI. When LPI was added to HEK 293 cells, which genetically modified overexpressed GPR55, ERK1⁄2 (extracellular - signal regulated kinase) was phosphorylated. The stimulation of LPI also induced a transient increase of intracellular Ca^2+ in HEK 293. These effects were specific to LPI and this study reported LPI as an endogenous ligand for GPR55 for the first time. Other potential ligands, which were also tested in this study, were not able to activate GPR55 (37). Since then, many other studies could show that LPI induces intracellular Ca^2+ elevation (34).

LPI has a well-documented effect on cell migration. It has been reported that GPR55 activated by LPI induces the directional migration of human peripheral blood neutrophils (30).

The main intracellular target for the intracellular pathway of GPR55⁄LPI is ERK 1⁄2.

ERKs, extracellular signal - regulated kinase, are intracellular enzymes that are activated by phosphorylation. The phosphorylation of ERK1⁄2 as an effect of LPI stimulation was reported from many different cells expressing GPR55, for example prostate cancer cells, ovarian cancer cells and osteoclasts (34). Another intercellular target for LPI/GPR55 is the small GTPase Rho. It also activates the RhoA and ROCK leading to the induction of several transcription factors, altering the cellular physiology.

All these results taken together show that the intracellular signalling pathway of LPI/GPR55 leads to the activation of potent enzymes and transcription factors that are able to influence the cell metabolism, leading to altered gene expression, enhanced migration, and proliferation.

In 2011, Fonseca suggested that the LPI/GPR55 axis plays a crucial role in foetoplacental development. His research data provides evidence that GPR55 and LPI are involved in immunology, apoptosis, differentiation and migration of uterine cells during pregnancy in rodents (29).

In human placental tissue, mRNA of GPR55 was isolated but its function remains unclear. We analysed the effect of oxygen on the expression of GPR55 in first trimester placentas. Since GPR55 may regulate cell migration, we expected to see that higher oxygen concentrations than the physiologically low levels during the first trimester would lead to higher expression of GPR55. Elevated expression of GPR55 could enhance migration of extravillous trophoblasts, which regulate the blood supply from the uterine spiral arteries. The high oxygen concentrations could be a trigger for GPR55 expression to increase, in order to enhance the migration rate of extravillous trophoblast cells.

We also analysed the effect of LPI on the expression of GPR55. We expected to see a down regulation of GPR55 after prolonged stimulation with LPI. This way of regulation was already reported by a study published in 2012, where GPR55 was down regulated in HEK 293 cells after prolonged stimulation with LPI (28).

Matrix Metalloproteases are proven to be very important for angiogenesis and migration. It is interesting to see how MMPs react on different oxygen concentrations in placental tissue. MMPs are involved in invasion of extravillous trophoblastic cells into the uterine wall towards the spiral arteries.
A higher expression of MMPs in extravillous trophoblast cells would be plausible, since the onset of the maternal blood flow into the intervillous space was described to result in oxidative stress for the placenta. This rise in oxygen tension was proposed to be a trigger for the differentiation of invasive trophoblast cells (13). Extravillous trophoblast cells express MMP in order to reach the spiral arteries, where they could decrease the oxidative stress by building intra-arterial plugs.

Methods

I have obtained first trimester placentas from women undergoing elective pregnancy termination of nonmedical reason. All women were informed and signed a consent form agreeing to donate the placenta for scientific research use.

The placentas between gestational week 7 and 8 were transported by the emergency service from the gynaecologist to the histological department in culture medium (DMEM) to keep the tissue alive. In the histological laboratory the placentas were registered with an anonymous identification number (sample ID). The explant culture of the placentas was performed on the same day as the abortion took place.

Explant Culture

I worked with the placenta villous tissue under sterile conditions. The placentas where handled in a workbench under air current to avoid contamination. Hands were washed and disinfected gloves and lab coats where worn the whole time. The workplace and the instruments were cleaned and disinfected with 75% alcohol solution before and after every procedure.

Before I started the explant culture, the placentas were transferred from the transporting container into a culture dish containing PBS buffer.
I then examined the condition of the tissue through a microscope. Only the tissue which arrived at the institute in good condition could be used for the experiment and was then put into another culture dish and DMEM(Dulbecco´s Modified Eagle Medium: Nutrient Mixture F-12) /Haems F-12 (1:1) solution containing 1% Penicillin/Streptomycin, 1% Amphotericin B, 10% foetal calf serum and 2mM L-Glutamine was added. I dissected 48 small pieces of the placenta with a scalpel.
Four 12-well plates were prepared for one placenta and were indicated with the placentas sample ID.
Each of the four well plates was considered for a defined oxygen concentration.
2ml of the culture medium was put into each well and LPI was added to three wells of each plate.
I then transferred two pieces of the dissected tissue into each well of the well plates.
Finally, I put the well plates into the hypoxic workbench which was set up for 2.5%, 8% and 12% oxygen. The well plate, which was supposed to be incubated under 21% oxygen, was put into a different incubator under aerial oxygen. Additionally to the oxygen and LPI concentration, all cells were cultured under 5% CO_2 and 37°C.
After 48h of incubation the samples were subjected to RNA isolation procedure.

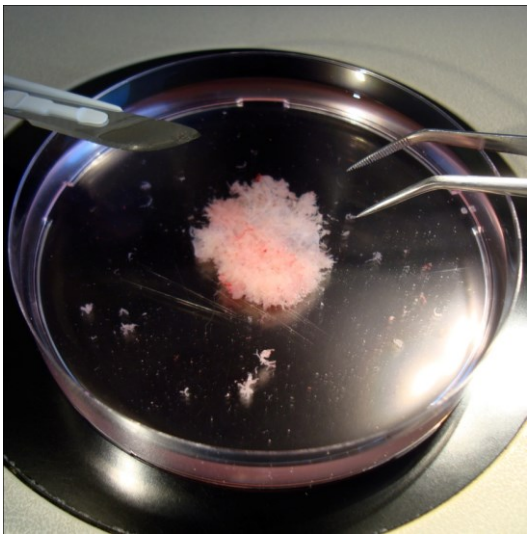

Figure 4, shows a sample of villous placental tissue obtained from first trimester after pregnancy termination

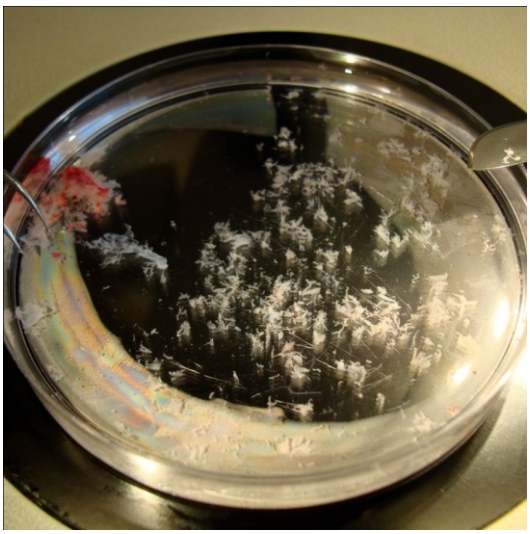

Figure 5, shows placental tissue being dissected into smaller pieces

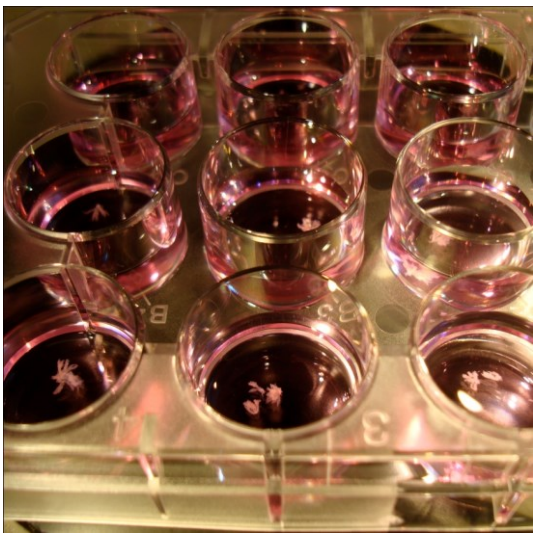

Figure 6, shows the small tissue pieces in a culture dish, ready for incubation

RNA Extraction

The next step was to homogenise the tissue which underwent incubation.
Therefore, I transferred the explant samples from the well plates into Eppendorf tubes containing 500µl of Trizol. Samples, which were incubated under identical conditions, were put together in one Eppendorf tube. So, for each placenta I obtained 8 Eppendorf tubes.
In order to homogenise the samples within the Trizol reagent, the Eppendorf tubes were mixed by a tissue homogeniser.
Before the Eppendorf tubes containing the tissue samples were stored in a freezer, they were clearly marked with the placenta ID, the date, the oxygen concentration under which the sample was incubated and weather LPI was present or not. The samples were stored at -80°C.
The Tri-reagent (Trizol) I used contains guanidine thiocyanate, which lyses cell membranes and denatures proteins. It is therefore able to inhibit RNase activity. Ribonucleases are enzymes which are present in every cell and can destroy the RNA. So the elimination of the RNases is crucial to the success of the RNA isolation. Trizol also contains phenol, in which proteins and nucleid acids can get dissolved.

To isolate the RNA, I used the single step method introduced by Piotr Chomczynski and Nicoletta Sacchi in 1987 as `guanidinium thiocyanate phenol chloroform extraction´.
This method consists of two steps, in the first step the cell membranes get lysed, so that the cells contents are set free in the solution. Next the RNA are separated from other cell components, so that it can be precipitated.

The Eppendorf tubes were defrosted, which took approximately half an hour. Then 100µl of BCP was added to every tube.
By adding 1-Bromo-3-Chloropropane (BCP) and shaking, the homogenate was separated into aqueous and organic phases.
The samples were incubated at room temperature for 15 minutes and finally were centrifuged at 12000g for 15 minutes at 4°C.
After centrifugation, the separation of the phases became visible.
The colourless aqueous upper phase contained exclusively RNA, the interphase contained DNA, and proteins dissolved in phenol and lipids dissolved in chloroform remain in the organic phase on the bottom of the E-Cup.

Then I pipetted the aqueous phase into a new E-Cup carefully as not to also transfer any of the other phases into the new E-Cup.
To precipitate RNA from the aqueous phase, I added 1000µl Isopropanol to the supernatant.
Then I shook the E cups and waited for 10 minutes. After another centrifugation at 12000g for 8min at 4°C, the RNA became visible at the bottom or side of the E-Cup as a white pellet.

I then carefully poured out the supernatant so that only the RNA pellet remained in the E-cup.
In order to wash the RNA pellet from any residues, I added 1ml of Ethanol to the cup.
Then I put the E-Cups into the centrifuge at 7.500g for 5min at 4°C to fixate the pellet on the bottom of the Cup.
Afterwards, I removed the ethanol, again carefully not to lose the pellet and then left the RNA pellet at room temperature to dry for 5min.
Finally, I dissolved the RNA pellet by adding 30µl RNase free distilled water and by passing the solution a few times through a pipette tip. Then I put the samples into the thermal shaker for 5 minutes at 55°C.
The isolated RNA samples were stored on ice for the following RNA measurement.

RNase contamination is a major problem during isolation of RNA, since these enzymes are ubiquitously present and can rapidly degrade RNA. Therefore, gloves were worn throughout the procedure and tubes were closed when not used.

Measurement of RNA concentration

To measure the quantity of isolated RNA and for purity control, I used the spectral photometer Nano Drop ND-1000 from PEQLAB.
To measure the concentration of isolated RNA in the solution the principle of spectralanalysis of absorptions is used.
The photometer sends short-wave light through the solution and then measures the absorption of the transmitted light. Beer - Lamberts´ law allows calculating the concentration of the substance (RNA) in the solution.
For purity control, the quotient of the absorption data at 260 and 280 nm is built. Values smaller than 2 reflect contamination of the sample by proteins or phenoles, whereas values around 2

imply residue-free, pure RNA.
For calibration, I first measured the absorption of the solvent: 1,5µl of RNase free distilled water, which was used to dissolve the RNA. Then I pipetted 1.5µl of each sample onto the scanner for concentration analysis. After each measurement, I cleaned the scanner with aqua dest on lint-free cloth, to avoid the contamination of the samples with each other. The results of the concentration analysis were indicated by the computer in a graph diagram.

Reverse Transcription: from RNA to cDNA by SuperScript 2 Reverse Transcriptase

The isolated RNA needed to be transcribed into cDNA in order to be able to perform qPCR.
cDNA is the term for complementary DNA, which is transcribed from RNA by two enzymes. First, a reverse transcriptase is needed; this enzyme is able to synthesize a complementary cDNA strand to a RNA template. The reverse transcriptase needs a short complementary strand, the primer, attached to the RNA template strand in order to start the synthesis of cDNA. The enzyme attaches the complementary DNA bases to their RNA complements.
The first product of the synthesis is a cDNA/RNA mixed strand, of which the residual RNA strand needs to be hydrolysed, so that a single stranded cDNA is left.
This remaining cDNA strand then serves as the template for the second enzyme, the DNA depending polymerase. The DNA polymerase adds the second cDNA strand, which results in a double stranded cDNA strand, which can be used for qPCR.

I used the enzyme SuperScript 2 Reverse Transcriptase (SS2 RT), which is an engineered version of M-MLV RT (Moloney Murine Leukemia Virus Reverse Transcriptase). SS2 RT is purified from E.coli and provides increased thermal stability and reduced RNase H activity.
The enzyme SS2 RT is an RNA-depending DNA polymerase, which also needs a small complementary strand, called primer, to start the transcription, as described above.
The product of SS2 RT is a single strand of cDNA hybridised with the initial RNA strand.
To degrade the remaining RNA strand I used the enzyme RNase H.

To 2µg of the initially isolated RNA I added 1µl Oligo(dT) and 1µl dNTP Mix into a nuclease-free microcentrifuge tube and filled it up with sterile, distilled water up to 12µl.
Then I heated the mixture for 5 min to 65°C and then quickly chilled it on ice. Afterwards, I collected the contents of the tube by brief centrifugation.

Next, I added 5X First-Strand Buffer (4µl), 0.1 M DTT (2µl) and RNase OUT (40 units/µl) to the tubes, mixed them gently and then incubated the samples for 2 min at 42°C.

Afterwards, I added 1µl (200 units) of SuperScript2 RT and mixed with a pipette by passing the solution a few times through the tip.

Finally I incubated the mixture at 42°C for 50 min and then I terminated the reaction by heating it up to 70°C for 15 min in a thermal cycler.

I diluted the resulting cDNA up to 200µl by adding 180µl of Aqua-dest.

Quantitative Real time Polymerase Chain Reaction

The goal of the qPCR was to measure how much mRNA of the target genes was expressed in the initial placental explants. The amount of isolated mRNA tells us about the transcription activity in the cells we exposed to the O2 concentrations and LPI.

In order to measure the quantity of the isolated RNA, I used qPCR.

Quantitative PCR works with the classical PCR mechanism, which was introduced by Kary Mullis in 1983. The difference is that with this method, the targeted cDNA is quantified simultaneously to the amplification(38).

The qPCR process takes place in a thermal cycler. This machine is able to rapidly heat and chill the samples according to the stages of the amplification process. Additionally, the qPCR thermal cycler can illuminate the samples with a specific wave length to detect the fluorescence emitted by the amplified cDNA product.

During the PCR process, serial temperature changes are repeated. In each cycle there are three different temperature stages. The reaction starts at 95°C, at this temperature the DNA melting takes place. The nucleid acid double chain separates as the hydrogen bonds between the complementary bases are disrupted. At 50-60°C in the next step the alignment of the primers with the single stranded cDNA templates takes place. Hydrogen bonds are formed between the DNA template and the primer. At this step, the DNA polymerase also already attaches to the primer. Finally, at 68-72°C, the polymerase starts at the 3' end of the primer to fill up the matching nucleotides to yield the synthesis of a complementary DNA strand(24).

This cycle is repeated about 40 times.

At the beginning of PCR, a chain reaction is set in motion, in which the produced DNA serves itself as a template for the replication in the next cycle. Until the reaction is slowed down, the DNA template is exponentially amplified. The reaction is determined by the available substrates, since

they are consumed in every cycle they become limiting to the reaction and the PCR slows down.

To perform qPCR the cDNA of each sample needed to be mixed with a Mastermix containing a taq Polymerase, which is an enzyme originally isolated from the Thermus aquaticus, a bacterium living in hot springs. This enzyme is able to synthesise DNA at high temperatures, which is necessary in PCR. The Mastermix also contains nucleotides (dNTPs), the building components for the reaction, a buffer solution providing a suitable chemical environment for the taq Polymerase,
divalent cations, magnesium ions and monovalent cations potassium ions.
Primers, complementary to the target region are also needed for the selective amplification of the cDNA sequences of interest.
The primers and the contents of the Mastermix provide the key components to enable selective and repeated amplification.

For every gene that I analysed, a specific primer was needed for the PCR amplification. So I prepared five Mastermix solutions, each with a specific primer for MMP 2,7,9,19 and GPR55.
At first I added 99µl of the primer containing solution to 990µl of the Mastermix and 396 µl of distilled DNase free water into a 2ml Eppendorf Cup. Then, I closed the cup and mixed it gently.
Then I labelled 40 small Eppendorf tubes for the next step. From each cDNA sample I pippeded 11µl into the labelled tubes and added 33µl of the prepared Mastermix containing the specific primer. I closed these tubes, mixed them gently and centrifuged them quickly.
Now all the components needed for PCR were combined in the tubes. So I pipetted 40µl of every tube into two wells of a 96 well plate (20µl per well), since the samples were analysed in duplicates. During all these steps, the tubes were cooled on ice blocks.
Finally, I sealed the plate with a sticky plastic foil and centrifuged it (600rpm/1min) before I put them into the PCR machine.

qPCR Taq Man Chemistry

During the process of amplification, the Taq Man Chemistry Technique allows a simultaneous quantification of the PCR product.

The Taq Man Probe consists of an oligonucleotide, which is labelled with a fluorescent dye at the 5`end. The fluorescent emission is erased by a quencher, which is attached to the 3`end of the probe. This Taq Man molecule connects to the present target sequence and is cleaved by the taq DNA polymerase during extension.

This decomposition of the Taq Man Probe separates the quencher from the dye and therefore, the fluorescent emission increases. The more amplification takes place, the more Taq Man Probes are separated from their target sequence and the more fluorescent is emitted. The fluorescent intensity is proportional to the amount of PCR product(38).

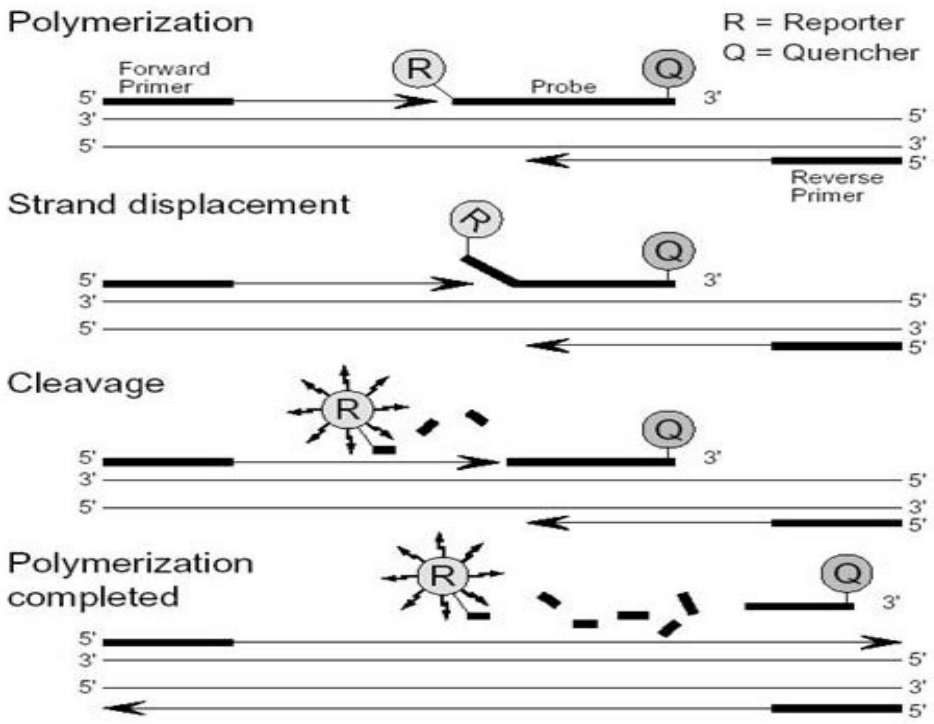

Figure 7, shows how the Taq Man Probe releases the dye (Reporter), which starts the fluorescence, when the probe is broken down by the polymerization. Picture from the internet: http://www.e-oligos.com/eoweb/products/eo-taqman.asp

qPCR analysis

The fluorescence emission is represented by an S-shaped graph in a diagram. In this graph diagram, one can display the accumulation of PCR products. There are three phases to be seen in the course of the graph. During the second phase, the PCR proves exponential amplification since all the reagents are available. In this phase, the PCR product is doubled in each cycle. Then the amplification slows down because some of the reagents are consumed by the reaction and the PCR product cannot be doubled at each cycle anymore thus the graph reaches a plateau(39).

In real time PCR the measurement takes place during the exponential phase. First, the point is measured when the fluorescence emission of a sample reaches intensity above the background fluorescence. This level of detection is called threshold. The so called threshold cycle (CT) is a precise PCR cycle during which the function value of a sample exceeds the threshold. Therefore, the CT value of a sample represents the beginning of exponential amplification. Values from the exponential amplification phase provide the most accurate and precise data for quantification.

The earlier the function value of a sample exceeds the threshold, the smaller is the CT value and the more cDNA is present in the sample(38).

Since the probes were analysed in duplicates, I calculated the mean CT value for each sample.

The CT mean values were further analysed by relative quantification.

Relative quantification

Relative quantification means that not the exact number of m RNA molecules in the probes at the start of the PCR process is calculated but the expression of the target gene is compared to the expression of a reference gene. In order to perform relative quantification, I compared the CT values from the target gene samples (MMPs/GPR55) to the CT values of the housekeeping gene RPL30.

Housekeeping genes are constitutive genes that code for proteins, which are necessary to maintain basic cellular function. They are expressed in all cells of an organism in physiological and pathophysiological condition. The RPL30 gene I used encodes a ribosomal protein, that is component of the 60s ribosomal subunit(38).

To calculate the ratio between the compared expressions, I used the ΔΔ Ct method.

ΔCt =	Ct target gene - Ct housekeeping gene
ΔΔCt =	ΔCt (LPI+) - ΔCt (LPI-)
Ratio =	2 ^ - ΔΔ Ct

Table 1, shows the calculation steps of the ΔΔCt method for relative quantification.

The Delta CT (ΔCt) value is the result from subtracting the CT values of target genes from the CT values of the housekeeping gene.

ΔΔCt method

With the help of the ΔΔCT values the target gene samples can be compared with each other. Hence, two values of samples of different condition (LPI+/LPI-) can be compared and the ratio is calculated by the following equation: n-fold expression = $2^{-\Delta\Delta Ct}$ (treated versus untreated).

Results

Statistical analysis

Box plots and Shapiro-Wilk Test of normal distribution

Statistical significance of differences in gene expression between different treatments was calculated using ΔCt values of different treatments. First, we utilised boxplots to visualise the medians and interquartile ranges of the ΔCt values. The boxes reach from the 25^th to the 75^th percentile and the line in the box indicates the median. Whiskers extending vertically from the boxes indicate variability outside the upper and lower quartiles. Since boxplots are non-parametric, they do not make any assumption about the statistical distribution of the samples.

However, to be able to choose a suitable statistical test for the variables, it is necessary to know if the ΔCt variables are normally distributed, since many statistical tests are only applicable for normally distributed variables.

Therefore, we used the Shapiro-Wilk test, which was first described in 1965 by Samuel Shapiro and Martin Wilk(40). This test analyses the null hypothesis that the samples come from a normally distributed population. Our ΔCt values come from a small sample number (n=5 per treatment), which can cause impreciseness in the statistical analysis due to the high standard error. The Shapiro-Wilk test is suitable to analyse these ΔCt values because compared to different tests of normal distribution, the Shapiro-Wilk test is able to work with a small sample ($3<n<50$) with high sensitivity. The Shapio-Wilk test only allows to determine whether the ΔCt values are normally distributed or not, it does not give any information about skewness of not normal distributed ΔCt values.(40)

The alpha level was chosen at 0.05. So, if the p value is greater than the alpha level ($p > 0.05$), the null hypothesis is not rejected and the samples are seen as normally distributed.

Firstly, we evaluated the samples for each 0_2 concentration and compared the samples with LPI (LPI+) the samples without LPI (LPI-).

For the comparison LPI+/LPI- normally distributed are the following ($p>0.05$):

Oxygen = 2.5 %
ΔCt for: MMP7, MMP9, MMP19, GRP55 (all except MMP2)

Oxygen = 8 %
ΔCt for all genes

Oxygen = 12 %
ΔCt for all genes

Oxygen = 21 %
ΔCt for MMP9 and GPR55

Secondly, we analysed the ΔCt values of all samples, which contained LPI (LPI+) and compared the different oxygen concentrations, then we did the same evaluation for all samples, which did not contain LPI (LPI-).
For the comparison of different O_2-concentrations normally distributed are the following ($p>0.05$):

LPI+
deltaCt for: MMP7, MMP9, MMP19, GRP55 (all except MMP2)

LPI-
deltaCt for MMP9, GPR55

For these ΔCt values, which were normally distributed, we used the students' t test to compare two independent, normal distributed samples. To compare more than two independently, normally distributed samples we used the single factor variance analysis ONEWAY ANOVA.

Statistical analysis for MMP2

The statistical analysis of the ΔCt values for MMP2 did not show any significant correlation between different oxygen concentrations, LPI and the expression of MMP2.

The p values from the student´s t-tests and the ANOVA analysis were all higher than the chosen level of significance > 0.05 and indicated therefore no significant results.

Effect of oxygen on MMP2 expression, results for LPI-

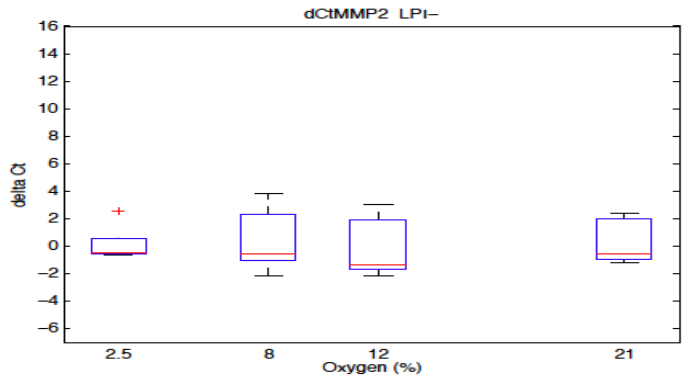

Oxygen	Mean	Std. Dev.	Median	Minimum	Maximum	n
2.5	0.16613	1.356	-0.50008	-0.61202	2.5587	5
8	0.44221	2.3529	-0.5814	-2.1543	3.7986	5
12	-0.10915	2.2514	-1.342	-2.1476	3.0146	5
21	0.34272	1.6713	-0.52372	-1.2166	2.3992	5

Figure 8, shows the ΔCts of MMP2 expression in different oxygen concentrations, when LPI is not present.

Effect of oxygen on MMP2 expression, results for LPI+

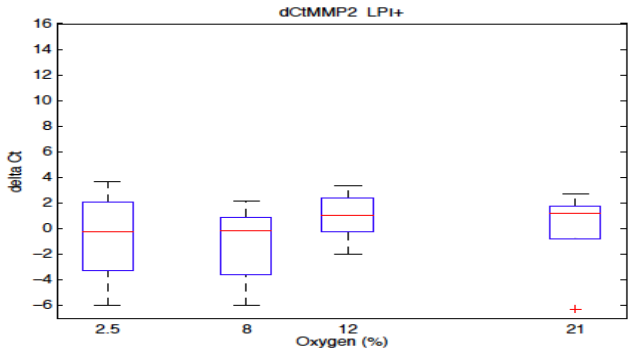

Oxygen	Mean	Std. Dev.	Median	Minimum	Maximum	n
2.5	-0.70886	3.6934	-0.28306	-6.002	3.6178	5
8	-1.2611	3.2007	-0.16207	-6.0433	2.1455	5
12	0.96479	2.0082	1.0601	-1.9991	3.3846	5
21	0.042473	3.6131	1.2227	-6.313	2.7456	5

Figure 9, shows the ΔCts of MMP2 expression in different oxygen concentrations, under the influence of LPI.

Effect of LPI on MMP2 expression, results for Oxygen 2.5%

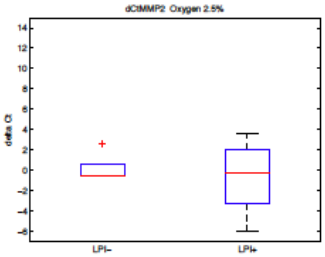

lpi	Mean	Std.	Med.	Min.	Max.	n
LPI-	0.16613	1.356	-0.50008	-0.61202	2.5587	5
LPI+	-0.70886	3.6934	-0.28306	-6.002	3.6178	5

Figure 10, shows the effect of LPI on MMP2 expression under the influence of 2.5% oxygen.

Effect of LPI on MMP2 expression, results for Oxygen 8%

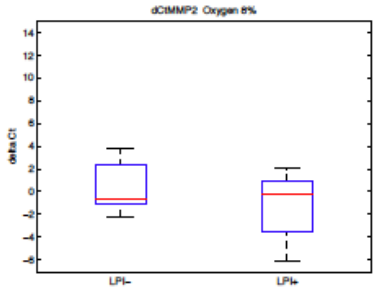

lpi	Mean	Std.	Med.	Min.	Max.	n
LPI-	0.44221	2.3529	-0.5814	-2.1543	3.7986	5
LPI+	-1.2611	3.2007	-0.16207	-6.0433	2.1455	5

Figure 11, shows the effect of LPI on MMP2 expression under the influence of 8% oxygen
e

Effect of LPI on MMP2 expression, results for Oxygen 12%

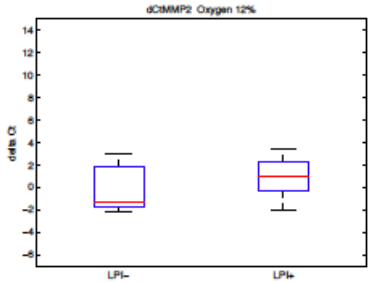

lpi	Mean	Std.	Med.	Min.	Max.	n
LPI-	-0.10915	2.2514	-1.342	-2.1476	3.0146	5
LPI+	0.96479	2.0082	1.0601	-1.9991	3.3846	5

.**Figure 12**, shows the effect of LPI on MMP2 under the influence of 12% oxygen

Effect of LPI on MMP2 expression, results for Oxygen 21%

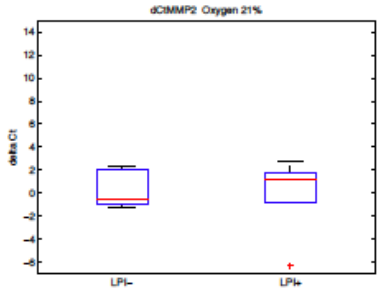

lpi	Mean	Std.	Med.	Min.	Max.	n
LPI-	0.34272	1.6713	-0.52372	-1.2166	2.3992	5
LPI+	0.042473	3.6131	1.2227	-6.313	2.7456	5

Figure 13, shows the effect of LPI on MMP2 under the influence of 21% oxygen

Student´s t-test for MMP2 in 8% oxygen:

		mean value	N	standard deviation	standard error of mean value
pair 1	MMP2	.44222600	5	2.352903354	1.052250369
	LPI_MMP2	-1.26111800	5	3.200751157	1.431419433

paired sample test

paired differences					T	df	significance, bilateral
mean value	standard deviation	standard error of mean value	95% confidence interval for mean difference				
			lower	upper			
1.703344000	1.821018258	.814384123	-.557748811	3.964436811	2.092	4	.105

Table 2, shows the students' t-test results for MMP2 under the influence of 8% oxygen. The p value is 0.105 > 0.05 which indicates no significant difference in expression.

Students' t-test for MMP2 in 12% oxygen:

		mean value	N	standard deviation	standard error of mean value
pair 1	MMP2	-.10914000	5	2.251370078	1.006843307
	LPI_MMP2	.96478400	5	2.008242051	.898113148

paired sample test

paired differences					T	df	significance, bilateral
mean value	standard deviation	standard error of mean value	95% confidence interval for mean difference				
			lower	upper			
-1.073924000	1.444933307	.646193820	-2.868045667	.720197667	-1.662	4	.172

Table 3, shows the result of the students' t-test for MMP2, under the influence of 12% oxygen. The p value is 0.172 >0.05 which indicates no significance in gene expression.

Statistical analysis for MMP7

The statistical analysis of the ΔCt values for MMP7 did not show any significant correlation between different oxygen concentrations, LPI and the expression of MMP7.

The p values from the students' t tests and the ANOVA analysis were all higher than the chosen level of significance > 0.05 and indicated therefore no significant results.

Effect of oxygen on MMP7 expression, results for LPI-

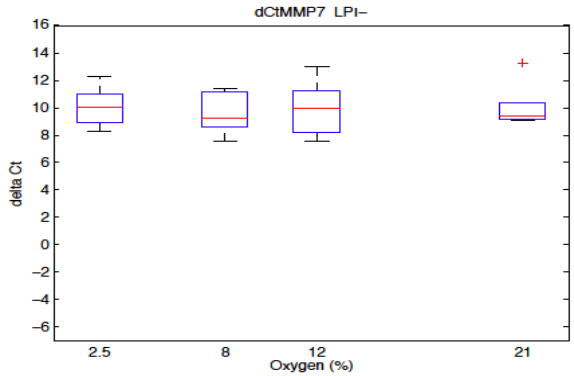

Oxygen	Mean	Std. Dev.	Median	Minimum	Maximum	n
2.5	10.055	1.5003	10.0166	8.3145	12.2402	5
8	9.6295	1.5886	9.2319	7.5494	11.329	5
12	9.9004	2.1147	9.9771	7.554	12.9801	5
21	10.0498	1.805	9.3531	9.0629	13.27	5

Figure 14, shows the effect of the different oxygen concentrations on the expression of MMP7, without LPI.

Effect of oxygen on MMP7 expression, results for LPI+

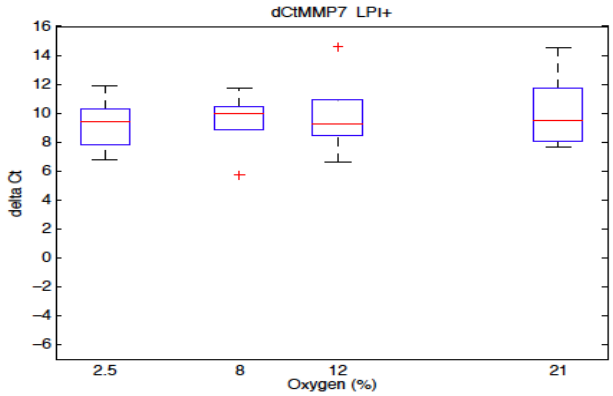

Oxygen	Mean	Std. Dev.	Median	Minimum	Maximum	n
2.5	9.1837	1.8929	9.3864	6.8172	11.8856	5
8	9.455	2.2327	9.9353	5.7026	11.7152	5
12	9.8266	2.9062	9.2387	6.6092	14.5679	5
21	10.1254	2.7333	9.4989	7.6775	14.507	5

Figure 15, shows the effect of the different oxygen concentrations and LPI on the expression of MMP7.

Effect of LPI on MMP7 expression, results for Oxygen 2.5%

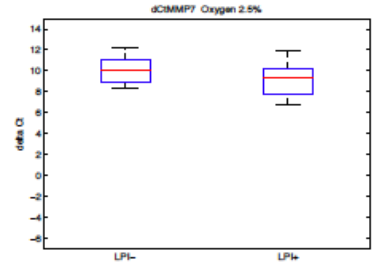

lpi	Mean	Std.	Med.	Min.	Max.	n
LPI-	10.055	1.5003	10.0166	8.3145	12.2402	5
LPI+	9.1837	1.8929	9.3864	6.8172	11.8856	5

Figure 16, shows the effect of LPI on the expression of MMP7 under the influence of 2.5% oxygen.

Effect of LPI on MMP7 expression, results for Oxygen 8%

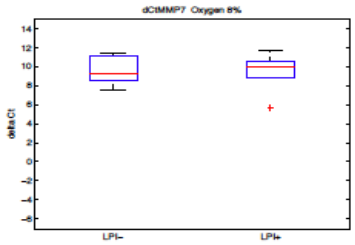

lpi	Mean	Std.	Med.	Min.	Max.	n
LPI-	9.6295	1.5886	9.2319	7.5494	11.329	5
LPI+	9.455	2.2327	9.9353	5.7026	11.7152	5

Figure 17, shows the effect of LPI on the expression of MMP7 under the influence of 8% oxygen.

Effect of LPI on MMP7 expression, results for Oxygen 12%

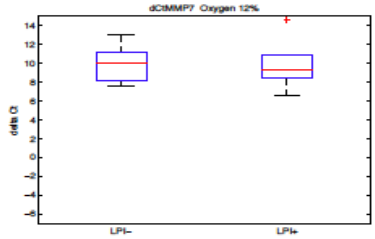

lpi	Mean	Std.	Med.	Min.	Max.	n
LPI-	9.9004	2.1147	9.9771	7.554	12.9801	5
LPI+	9.8266	2.9062	9.2387	6.6092	14.5679	5

Figure 18, shows the effect of LPI on the expression of MMP7 under the influence of 12% oxygen.

Effect of LPI on MMP7 expression, results for Oxygen 21%

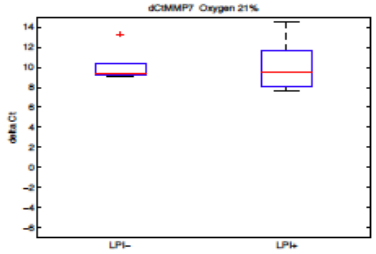

lpi	Mean	Std.	Med.	Min.	Max.	n
LPI-	10.0498	1.805	9.3531	9.0629	13.27	5
LPI+	10.1254	2.7333	9.4989	7.6775	14.507	5

Figure 19, shows the effect of LPI on the expression of MMP7 under the influence 21% oxygen.

Students' t-test for MMP7 in 2.5% oxygen:

paired samples

		mean value	N	standard deviation	standard error of mean value
pair 1	MMP7	10.055020	5	1.5003194	.6709632
	LPI_MMP7	9.183700	5	1.8928582	.8465119

paired differences					T	df	significance, bilateral
mean value	standard deviation	standard error of mean value	95% confidence interval for mean difference				
			lower	upper			
.8713200	1.6433198	.7349149	-1.1691310	2.9117710	1.186	4	.301

Table 4, shows the result of the students' t-test for MMP7 under the influence of 2.5% oxygen. The p- value is 0.301 >0.05, which indicates no significant difference in expression.

Student´s t-test for MMP7 in 8% oxygen:

paired samples

		mean value	N	standard deviation	standard error of mean value
pair 1	MMP7	9.629500	5	1.5886409	.7104618
	LPI_MMP7	9.454960	5	2.2326703	.9984805

paired differences					T	df	significance, bilateral
mean value	standard deviation	standard error of mean value	95% confidence interval for mean difference				
			lower	upper			
.1745400	2.2530073	1.0075755	-2.6229380	2.9720180	.173	4	.871

Table 5, shows the result of the t-test for MMP7 under the influence of 8% oxygen. The p value is 0.871>0.05, which indicates no significant difference.

Students' t-test for MMP7 in 12% oxygen:

paired samples

		mean value	N	standard deviation	standard error of mean value
pair 1	MMP7	9.900400	5	2.1147004	.9457228
	LPI_MMP7	9.826600	5	2.9061572	1.2996730

paired differences					T	df	significance, bilateral
mean value	standard deviation	standard error of mean value	95% confidence interval for mean difference				
			lower	upper			
.0738000	1.5734386	.7036631	-1.8798821	2.0274821	.105	4	.922

Table 6, shows the result of the t-test for MMP7 under the influence of 12%oxygen. The p value is 0.922 > 0.05, which indicates no significant result.

Results of the ANOVA statistical analysis for MMP7

MMP7

	N	mean value	standard deviation	standard error	95%- confidence interval of mean value		minimum	maximum
					lower	upper		
2.5	5	9.183700	1.8928582	.8465119	6.833406	11.533994	6.8172	11.8856
8.0	5	9.454960	2.2326703	.9984805	6.682734	12.227186	5.7026	11.7152
12.0	5	9.826600	2.9061572	1.2996730	6.218129	13.435071	6.6092	14.5679
21.0	5	10.125420	2.7333137	1.2223751	6.731563	13.519277	7.6775	14.5070
in total	20	9.647670	2.2999000	.5142733	8.571284	10.724056	5.7026	14.5679

MMP7

	sum of squares	df	mean squares	F	significance
between groups	2.563	3	.854	.140	.935
within groups	97.938	16	6.121		
in total	100.501	19			

Table 7, shows the results of the ANOVA analysis of the ΔCt values of the expression of MMP7. The p value is 0.93 > 0.05 which indicates no significant difference.

Statistical analysis for MMP9

The statistical analysis of the ΔCt values for MMP9 did not show any significant correlation between different oxygen concentrations, LPI and the genetic expression of MMP9.

The p values from the students' t tests and the ANOVA analysis were all higher than the chosen level of significance > 0.05 and indicated therefore no significant results.

Effect of oxygen on MMP9 expression, results for LPI-

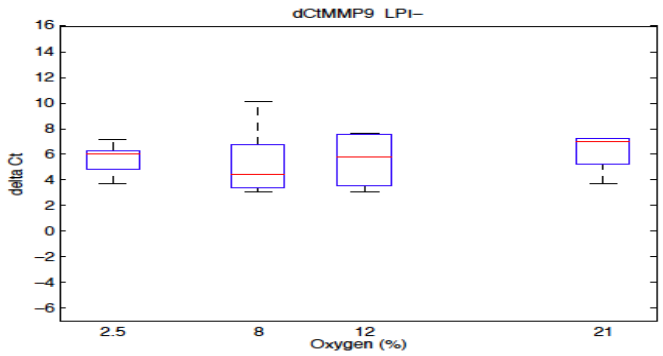

Oxygen	Mean	Std. Dev.	Median	Minimum	Maximum	n
2.5	5.6325	1.2709	6.0563	3.7255	7.1377	5
8	5.3455	2.8446	4.3981	3.0633	10.1053	5
12	5.5589	2.0876	5.7689	3.0977	7.6226	5
21	6.1914	1.5259	6.9878	3.6726	7.2622	5

Figure 20, shows the effect of the different oxygen concentrations on the expression of MMP9, without LPI.

Effect of oxygen on MMP9 expression, results for LPI+

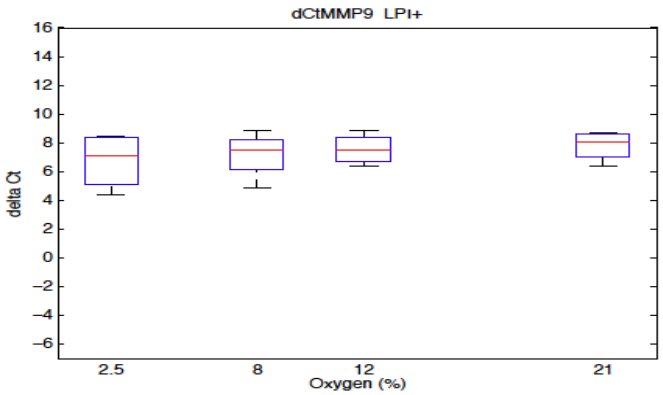

Oxygen	Mean	Std. Dev.	Median	Minimum	Maximum	n
2.5	6.7572	1.9452	7.0655	4.4244	8.4735	4
8	7.1711	1.6599	7.4817	4.8783	8.8425	4
12	7.5715	1.0769	7.4969	6.4148	8.8776	4
21	7.8128	1.071	8.1009	6.3896	8.6596	4

Figure 21, shows the effect of the different oxygen concentrations on the expression of MMP9 under the influence of

LPI.

Effect of LPI on MMP9 expression, results for Oxygen 2.5%

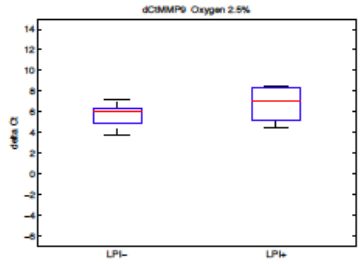

lpi	Mean	Std.	Med.	Min.	Max.	n
LPI-	5.6325	1.2709	6.0563	3.7255	7.1377	5
LPI+	6.7572	1.9452	7.0655	4.4244	8.4735	4

Figure 22, shows the effect of LPI on the expression of MMP9 under 2.5% oxygen.

Effect of LPI on MMP9 expression, results for Oxygen 8%

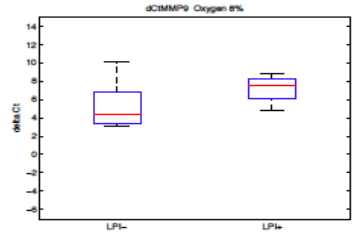

lpi	Mean	Std.	Med.	Min.	Max.	n
LPI-	5.3455	2.8446	4.3981	3.0633	10.1053	5
LPI+	7.1711	1.6599	7.4817	4.8783	8.8425	4

Figure 23, shows the effect of LPI on the expression of MMP9 under the influence of 8% oxygen.

Effect of LPI on MMP9 expression, results for Oxygen 12%

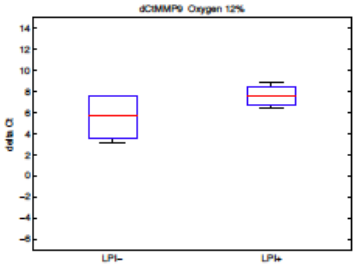

lpi	Mean	Std.	Med.	Min.	Max.	n
LPI-	5.5589	2.0876	5.7689	3.0977	7.6226	5
LPI+	7.5715	1.0769	7.4969	6.4148	8.8776	4

Figure 24, shows the effect of LPI on the expression of MMP9 under the influence of 12% oxygen.

Effect of LPI on MMP9 expression, results for Oxygen 21%

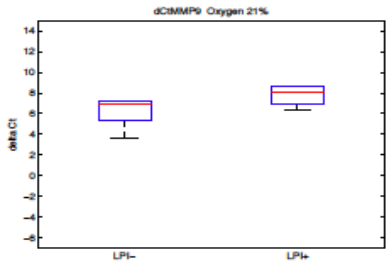

lpi	Mean	Std.	Med.	Min.	Max.	n
LPI-	6.1914	1.5259	6.9878	3.6726	7.2622	5
LPI+	7.8128	1.071	8.1009	6.3896	8.6596	4

Figure 25, shows the effect of LPI on the expression of MMP9 under the influence of 21% oxygen.

Students' t-test for MMP9 in 2.5 oxygen:

paired samples

		mean value	N	standard deviation	standard error of mean value
pair 1	MMP9	6.109250	4	.7990172	.3995086
	LPI_MMP9	6.757225	4	1.9452244	.9726122

paired samples

paired differences					T	df	significance bilateral
mean value	standard deviation	standard error of mean value	95% confidence interval for the mean difference				
			lower	upper			
-.6479750	1.9223513	.9611757	-3.7068649	2.4109149	-.674	3	.549

Table 8, shows the result of the t-test for MMP9 under the influence of 2.5% oxygen. The p values is 0.549 > 0.05, which indicates no significant result.

Students' t-test for MMP9 in 8% oxygen:

paired samples

		mean value	N	standard deviation	standard error of mean value
pair 1	MMP9	5.812625	4	3.0552318	1.5276159
	LPI_MMP9	7.171050	4	1.6598995	.8299498

paired differences					T	df	significance, bilateral
mean value	standard deviation	standard error of mean value	95% confidence interval of mean difference				
			lower	upper			
-1.3584250	3.0422528	1.5211264	-6.1993280	3.4824780	-.893	3	.438

Table 9, shows the result of the t-test for MMP9 under the influence of 8% oxygen. The p value is 0.438 > 0.05, which indicates no significant result.

Student´s t-test for MMP9 in 12% oxygen:

paired samples

		mean value	N	standard deviation	standard error of mean value
pair 1	MMP9	6.174175	4	1.8129886	.9064943
	LPI_MMP9	7.571525	4	1.0769392	.5384696

paired differences					T	df	significance, bilateral
mean value	standard deviation	standard error of mean value	95% confidence interval for the mean difference				
			lower	upper			
-1.3973500	1.2913441	.6456721	-3.4521666	.6574666	-2.164	3	.119

Table 10, shows the result of the t-test for MMP9 under the influence of 12% oxygen. The p value is 0.119 > 0.05, which indicates no significant result.

Students' t-test for MMP9 in 21% oxygen:

paired samples

		mean value	N	standard deviation	standard error of mean value
pair 1	MMP9	6.821100	4	.6789386	.3394693
	LPI_MMP9	7.812775	4	1.0710189	.5355095

paired differences					T	df	significance, bilateral
mean value	standard deviation	standard error of mean value	95% confidence interval for the mean difference				
			lower	upper			
-.9916750	.6417488	.3208744	-2.0128406	.0294906	-3.091	3	.054

Table 11, shows the result of the t-test under the influence of 21% oxygen for MMP9. The p value is 0.054 > 0.05, which indicates no significant result. However this result is the closest to the significance level we chose.

Results of the ANOVA statistical analysis for MMP9 with LPI

MMP9

	N	mean value	standard deviation	standard error	95%-confidence interval for mean difference		minimum	maximum
					lower	upper		
2.5	4	6.757225	1.9452244	.9726122	3.661939	9.852511	4.4244	8.4735
8.0	4	7.171050	1.6598995	.8299498	4.529779	9.812321	4.8783	8.8425
12.0	4	7.571525	1.0769392	.5384696	5.857874	9.285176	6.4148	8.8776
21.0	4	7.812775	1.0710189	.5355095	6.108545	9.517005	6.3896	8.6596
in total	16	7.328144	1.3932467	.3483117	6.585735	8.070553	4.4244	8.8776

MMP9

	sum of squares	df	mean squares	F	significance
between groups	2.579	3	.860	.389	.763
within groups	26.538	12	2.212		
in total	29.117	15			

Table 12, shows the results for the ANOVA statistical analysis for MMP9 under the different oxygen concentrations, ***with LPI***. The p value is 0.763 > 0.05, which indicates no significant result.

Results of the ANOVA statistical analysis for MMP9 without LPI

MMP9

	N	mean value	standard deviation	standard error	95%-confidence interval for mean difference		minimum	maximum
					lower	upper		
2.5	5	5.632500	1.2709344	.5683791	4.054427	7.210573	3.7255	7.1377
8.0	5	5.345540	2.8445866	1.2721378	1.813519	8.877561	3.0633	10.1053
12.0	5	5.558880	2.0876148	.9336097	2.966764	8.150996	3.0977	7.6226
21.0	5	6.191400	1.5258862	.6823971	4.296762	8.086038	3.6726	7.2622
in total	20	5.682080	1.8851938	.4215421	4.799782	6.564378	3.0633	10.1053

MMP9

	sum of squares	df	mean squares	F	significance
between groups	1.952	3	.651	.159	.923
within groups	65.574	16	4.098		
in total	67.525	19			

Table 13, shows the results for the ANOVA statistical analysis for MMP9 and the different oxygen concentrations, ***without LPI***. The p value is 0.923, which indicates no significant result.

Statistical analysis for MMP19

The statistical analysis of the ΔCt values for MMP19 did not show any significant correlation between different oxygen concentrations, LPI and the genetic expression of MMP19.

The p values from the students' t tests and the ANOVA analysis were all higher than the chosen level of significance > 0.05 and indicated therefore no significant results.

Effect of oxygen on MMP19 expression, results for LPI-

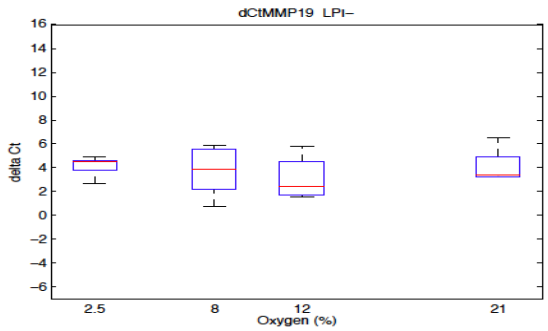

Oxygen	Mean	Std. Dev.	Median	Minimum	Maximum	n
2.5	4.1545	0.86258	4.4863	2.6883	4.8875	5
8	3.7398	2.1073	3.914	0.7204	5.8503	5
12	3.1433	1.7862	2.4324	1.5824	5.8135	5
21	4.1811	1.4114	3.3921	3.2626	6.5534	5

Figure 26, shows the effect of the different oxygen concentrations on the expression of MMP19, without LPI.

Effect of oxygen on MMP19 expression, results for LPI+

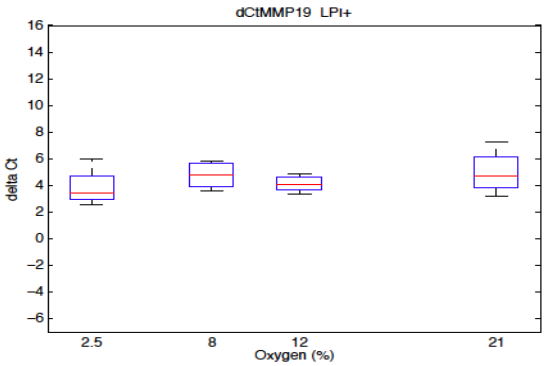

Oxygen	Mean	Std. Dev.	Median	Minimum	Maximum	n
2.5	3.8403	1.5001	3.4071	2.5414	6.0055	4
8	4.735	1.067	4.7544	3.5811	5.8499	4
12	4.1095	0.63282	4.0902	3.3868	4.8709	4
21	4.9671	1.6772	4.7401	3.1878	7.2005	4

Figure 27, shows the effect of the different oxygen concentrations on the expression of MMP19 under the influence of LPI.

Effect of LPI on MMP19 expression, results for Oxygen 2.5%

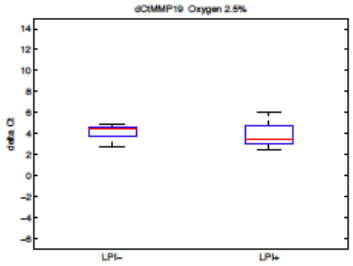

lpi	Mean	Std.	Med.	Min.	Max.	n
LPI-	4.1545	0.86258	4.4863	2.6883	4.8875	5
LPI+	3.8403	1.5001	3.4071	2.5414	6.0055	4

Figure 28, shows the effect of LPI on the expression of MMP19 under the influence of 2.5% oxygen.

Effect of LPI on MMP19 expression, results for Oxygen 8%

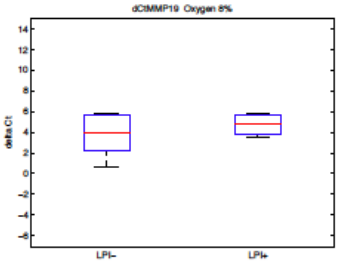

lpi	Mean	Std.	Med.	Min.	Max.	n
LPI-	3.7398	2.1073	3.914	0.7204	5.8503	5
LPI+	4.735	1.067	4.7544	3.5811	5.8499	4

Figure 29, shows the effect of LPI on the expression of MMP19 under the influence of 8% oxygen.

Effect of LPI on MMP19 expression, results for Oxygen 12%

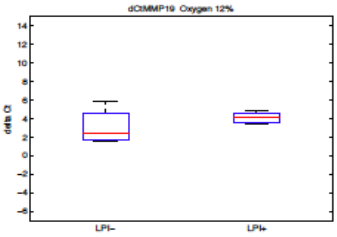

lpi	Mean	Std.	Med.	Min.	Max.	n
LPI-	3.1433	1.7862	2.4324	1.5824	5.8135	5
LPI+	4.1095	0.63282	4.0902	3.3868	4.8709	4

Figure 30, shows the effect of LPI on the expression of MMP19 under the influence of 12% oxygen.

Effect of LPI on MMP19 expression, results for Oxygen 21%

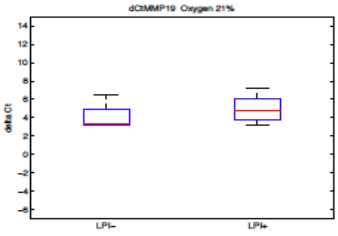

lpi	Mean	Std.	Med.	Min.	Max.	n
LPI-	4.1811	1.4114	3.3921	3.2626	6.5534	5
LPI+	4.9671	1.6772	4.7401	3.1878	7.2005	4

Figure 31, shows the effect of LPI on the expression of MMP19 under the influence of 21% oxygen.

Student´s t-test for MMP19 in 2.5% oxygen:

paired samples

		mean value	N	standard deviation	standard error of mean value
Pair 1	MMP19	4.521075	4	.3103263	.1551632
	LPI_MMP19	3.840275	4	1.5000622	.7500311

paired differences					T	df	significance, bilateral
mean value	standard deviation	standard error of mean value	95% confidence interval for the mean difference				
			lower	upper			
.6808000	1.4774099	.7387050	-1.6700889	3.0316889	.922	3	.425

Table 14, shows the result for the t-test for MMP19 under the influence of 2.5% oxygen. The p value is 0.425 > 0.05, which indicates no significant result.

Student´s t-test for MMP19 in 8% oxygen:

paired samples

		mean value	N	standard deviation	standard error of mean value
pair 1	MMP19	4.494650	4	1.4568259	.7284129
	LPI_MMP19	4.734950	4	1.0670155	.5335078

paired differences					T	df	significance, bilateral
mean value	standard deviation	standard error of mean value	95% confidence interval for mean difference				
			lower	upper			
-.2403000	1.8512111	.9256056	-3.1859900	2.7053900	-.260	3	.812

Table 15, shows the result for the t-test for MMP19 under the influence of 8% oxygen. The p value is 0.812 > 0.05, which indicates no significant result.

Students' t-test for MMP19 in 12% oxygen:

paired samples

		mean value	N	standard deviation	standard error of mean value
pair 1	MMP19	3.478775	4	1.8718773	.9359387
	LPI_MMP19	4.109550	4	.6328188	.3164094

paired differences					T	df	significance, bilateral
mean value	standard deviation	standard error of mean value	95% confidence interval for mean difference				
			lower	upper			
-.6307750	2.1928712	1.0964356	-4.1201225	2.8585725	-.575	3	.605

Table 16, shows the result for the t-test for MMP19 under the influence of 12% oxygen. The p value is 0.605 > 0.05, which indicates no significant result.

Results of the ANOVA statistical analysis for MMP19

MMP19

	N	mean value	standard deviation	standard error	95%-confidence interval for the mean difference		minimum	maximum
					lower	upper		
2.5	4	3.840275	1.5000622	.7500311	1.453341	6.227209	2.5414	6.0055
8.0	4	4.734950	1.0670155	.5335078	3.037090	6.432810	3.5811	5.8499
12.0	4	4.109550	.6328188	.3164094	3.102594	5.116506	3.3868	4.8709
21.0	4	4.967100	1.6771713	.8385857	2.298346	7.635854	3.1878	7.2005
in total	16	4.412969	1.2417545	.3104386	3.751284	5.074653	2.5414	7.2005

MMP19

	sum of squares	df	mean squares	F	significance
between groups	3.323	3	1.108	.671	.586
within groups	19.806	12	1.651		
in total	23.129	15			

Table 17, shows the results of the ANOVA statistical analysis for MMP19 and the different oxygen concentrations. The p value is 0.586 > 0.05, which indicates no significant result.

Statistical analysis for GPR55

The statistical analysis of the ΔCt values for GPR55 did not show any significant correlation between different oxygen concentrations, LPI and the expression of GPR55. Since LPI is the ligand for GPR55, its effect on the expression of GPR55 was most interesting.

However, the p values from the students' t tests and the ANOVA analysis were all higher than the chosen level of significance > 0.05 and indicated therefore no significant results.

Effect of oxygen on GPR55 expression, results for LPI-

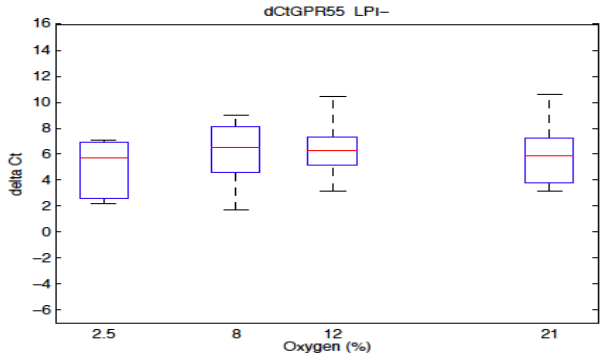

Oxygen	Mean	Std. Dev.	Median	Minimum	Maximum	n
2.5	4.928	2.3143	5.7328	2.2062	7.1025	5
8	6.1073	2.8	6.5249	1.6761	9.0126	5
12	6.404	2.5816	6.2733	3.1765	10.3961	5
21	5.9712	2.877	5.9134	3.1837	10.5991	5

Figure 32, shows the effect of the different oxygen concentrations on the expression of GPR55, without LPI.

Effect of oxygen on GPR55 expression, results for LPI+

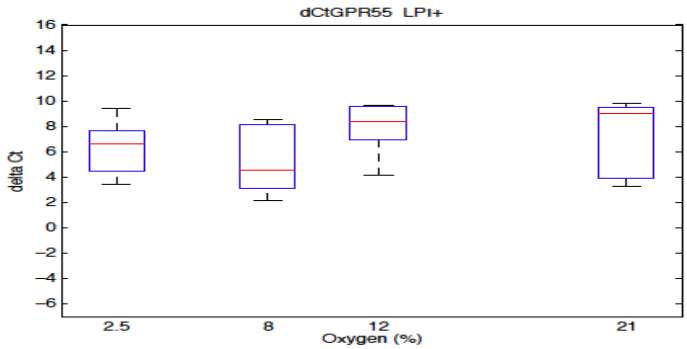

Oxygen	Mean	Std. Dev.	Median	Minimum	Maximum	n
2.5	6.2541	2.2787	6.6128	3.4438	9.4037	5
8	5.333	2.8183	4.5239	2.1619	8.5556	5
12	7.9245	2.2502	8.3481	4.1356	9.6743	5
21	7.1095	3.1679	9.0171	3.2832	9.8176	5

Figure 33, shows the effect of the different oxygen concentrations on the expression of GPR55 under the influence of LPI.

Effect of LPI on GPR55 expression, results for Oxygen 2.5%

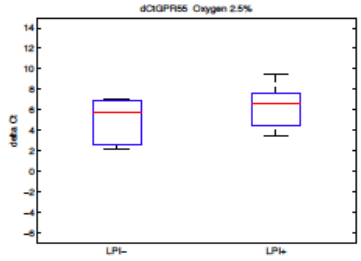

lpi	Mean	Std.	Med.	Min.	Max.	n
LPI-	4.928	2.3143	5.7328	2.2062	7.1025	5
LPI+	6.2541	2.2787	6.6128	3.4438	9.4037	5

Figure 34, shows the effect of LPI on the expression of GPR55 under the influence of 2.5% oxygen.

Effect of LPI on GPR55 expression, results for Oxygen 8%

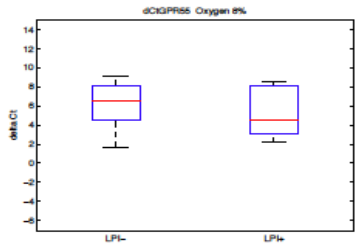

lpi	Mean	Std.	Med.	Min.	Max.	n
LPI-	6.1073	2.8	6.5249	1.6761	9.0126	5
LPI+	5.333	2.8183	4.5239	2.1619	8.5556	5

Figure 35, shows the effect of LPI on the expression of GPR55 under the influence of 8% oxygen.

Effect of LPI on GPR55 expression, results for Oxygen 12%

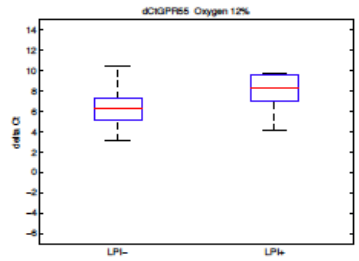

lpi	Mean	Std.	Med.	Min.	Max.	n
LPI-	6.404	2.5816	6.2733	3.1765	10.3961	5
LPI+	7.9245	2.2502	8.3481	4.1356	9.6743	5

Figure 36, shows the effect of LPI on the expression of GPR55 under the influence of 12% oxygen.

Effect of LPI on GPR55 expression, results for Oxygen 21%

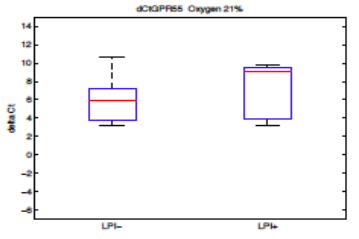

lpi	Mean	Std.	Med.	Min.	Max.	n
LPI-	5.9712	2.877	5.9134	3.1837	10.5991	5
LPI+	7.1095	3.1679	9.0171	3.2832	9.8176	5

Figure 37, shows the effect of LPI on the expression of GPR55 under the influence of 21% oxygen.

Students' t test for GPR55 in 2.5% oxygen:

paired samples

		mean value	N	standard deviation	standard error of mean value
pair 1	GPR55	4.928040	5	2.3143107	1.0349912
	LPI_GPR55	6.254120	5	2.2786959	1.0190638

paired differences					T	df	significance, bilateral
mean value	standard deviation	standard error of mean value	95% confidence interval for the mean difference				
			lower	upper			
-1.3260800	3.2359551	1.4471631	-5.3440490	2.6918890	-.916	4	.411

Table 18, shows the result of the t-test for GPR55 under the influence of 2.5% oxygen. The p value is 0.411 > 0.05, which indicates no significant result.

Students' t test for GPR55 in 8% oxygen:

paired samples

		mean value	N	standard deviation	standard error of mean value
pair 1	GPR55	6.107260	5	2.7999507	1.2521760
	LPI_GPR55	5.333000	5	2.8183396	1.2603998

tests for paired samples

paired differences					T	df	significance, bilateral
mean value	standard deviation	standard error of mean value	95% confidence interval for the mean difference				
			lower	upper			
.7742600	2.6118856	1.1680707	-2.4688243	4.0173443	.663	4	.544

Table 19, shows the result of the t-test for GPR55 under the influence of 8% oxygen. The p value is 0.544 > 0.05, which indicates no significant result.

Student´s t-test for GPR55 in 12% oxygen:

statistics for paired samples

		mean value	N	standard deviation	standard error of mean value
pair 1	GPR55	6.403960	5	2.5816370	1.1545431
	LPI_GPR55	7.924480	5	2.2501554	1.0063001

test for paired samples

paired differences					T	df	significance, bilateral
mean value	standard deviation	standard error of mean value	95% confidence interval for the mean difference				
			lower	upper			
-1.5205200	1.5745221	.7041477	-3.4755474	.4345074	-2.159	4	.097

Table 20, shows the result of the t-test for GPR55 under the influence of 12% oxygen. The p value is 0.097 > 0.05, which indicates no significant result.

Student´s t-test for GPR55 21% oxygen

statistics for paired samples

		mean value	N	standard deviation	standard error of mean value
pair 1	GPR55	5.971140	5	2.8769656	1.2866181
	LPI_GPR55	7.109460	5	3.1679394	1.4167456

Test for paired sample

paired differences					T	df	significance, bilateral
mean value	standard deviation	standard error of mean value	95% confidence interval for mean difference				
			lower	upper			
-1.1383200	4.7013050	2.1024875	-6.9757612	4.6991212	-.541	4	.617

Table 21, shows the result of the t-test for GPR55 under the influence of 21% oxygen. The p value is 0.617 > 0.05, which indicates no significant result.

Results of the ANOVA statistical analysis for GPR55 with LPI

GPR55

	N	mean value	standard deviation	standard error	95%-confidence interval for the mean difference		minimum	maximum
					lower	upper		
2.5	5	6.254120	2.2786959	1.0190638	3.424745	9.083495	3.4438	9.4037
8.0	5	5.333000	2.8183396	1.2603998	1.833569	8.832431	2.1619	8.5556
12.0	5	7.924480	2.2501554	1.0063001	5.130543	10.718417	4.1356	9.6743
21.0	5	7.109460	3.1679394	1.4167456	3.175944	11.042976	3.2832	9.8176
in total	20	6.655265	2.6314959	.5884204	5.423687	7.886843	2.1619	9.8176

GPR55

	sum of squares	df	mean square	F	significance
between groups	18.633	3	6.211	.880	.472
within groups	112.938	16	7.059		
in total	131.571	19			

Table 22, shows the results of the ANOVA statistical analysis for GPR55 and the different oxygen concentrations, with LPI. The p value is 0.472 > 0.05, which indicates no significant differences.

Results of the ANOVA statistical analysis for GPR55 without LPI

GPR55

	N	mean value	standard deviation	standard error	95%-confidence interval for the mean difference		minimum	maximum
					lower	upper		
2.5	5	4.928040	2.3143107	1.0349912	2.054444	7.801636	2.2062	7.1025
8.0	5	6.107260	2.7999507	1.2521760	2.630662	9.583858	1.6761	9.0126
12.0	5	6.403960	2.5816370	1.1545431	3.198434	9.609486	3.1765	10.3961
21.0	5	5.971140	2.8769656	1.2866181	2.398915	9.543365	3.1837	10.5991
in total	20	5.852600	2.4998812	.5589904	4.682620	7.022580	1.6761	10.5991

GPR55

	sum of squares	df	mean squares	F	significance
between groups	6.189	3	2.063	.293	.830
within groups	112.550	16	7.034		
in total	118.739	19			

Table 23, shows the result of the ANOVA statistical analysis for GPR55 and the different oxygen concentrations without LPI. The p value is $0.830 > 0.05$, which indicates no significant differences.

Discussion

The aim of this study was to detect a possible influence of different oxygen concentrations on the gene expression of MMPs and GPR55 in placental villous tissue. Additionally, I investigated whether LPI, the ligand of GPR55, has an influence on the expression of its receptor itself and on MMPs. The results indicate no significant influence of the different oxygen concentrations and/or LPI incubation on the mRNA amount of the encoding genes for GPR55 or the analysed MMPs.

A possible limitation of this study was the duration of incubation. The placental tissue was incubated only for 48 hours under the influence of LPI and the different oxygen concentrations. Placental cells might need more time under these non-physiological oxygen concentrations to react with altered gene expression of GPR55 and the MMPs. The influence of LPI might also need more time than 48 hours to cause a possible effect on the genetic expression of GPR55 or the MMPs.

Moreover, the analysed samples were pieces of whole placental tissue, so all types of placental cells, including trophoblasts, mesenchymal cells, foetal endothelial cells and Hofbauer cells were present in the sample. This sample was analysed in a culture medium, to which LPI was added. In this setting, LPI was probably not able to reach its receptor GPR55, which may in fact not be expressed in the villous trophoblast, representing the outmost layer of placental villi. Thus, LPI may not affect GPR55 expression in other placental cell types, since it was not able to cross the syncytiotrophoblast and reach its receptor on other placental cell types. In order to clarify this important point, localisation of GPR55 by immunohistochemistry is required in future studies.

The half live of LPI also has to be taken into consideration regarding the question whether LPI was able to reach its receptor in this setting. It is not known how stable the LPI molecule is in the culture medium. So again, time could be an issue regarding the half-life of LPI. If the LPI molecule degrades before it can bind to the GPR55 receptor, these results would not represent the influence of LPI on GPR55.

For further research, it would be interesting to discover which cells in the first term placenta are expressing MMP molecules. If only a small number of extravillous trophoblast cells express MMP enzymes, it could adulterate the gene expression analysis of this study. Since I analysed the isolated mRNA of all cells in the tissue sample, it is difficult to detect differences in genetic expression of only a few cells.

These extravillous trophoblastic cells would be most likely to express MMP enzymes since they

need to be able to splice the extravillous matrix to invade into the uterine wall.

However, during the process of protein biosynthesis, there are many steps that are open for regulation, for example the translation of the mRNA into the amino-acid sequence and the protein processing. It is important to take into consideration that I only investigated the mRNA amount of the MMPs and GPR55. Any possible regulation that takes place later in the protein biosynthesis than the transcription of the encoding genes into mRNA could not be detected by the RT PCR in this study.

MMPs are precisely regulated by protein processing and by specific inhibitors. They are secreted as proenzymes and need to be spliced, in order to be activated and are further regulated by specific inhibiting enzymes, the TIMPs. If oxygen concentrations different from the physiological level influence the amount of functional MMP secreted by a cell, this influence could alter the regulation mechanisms post transcriptional. At the post-transcriptional level, the expression of MMPs can be regulated by altered stability of the mRNA molecule (41).

I only investigated the relative quantity of mRNA molecules via RT PCR; however, no conclusions from these results can be made regarding the stability of the mRNA molecule. Studies could show that the regulation of the m RNA metabolism plays a major role in the control of gene expression(42). RNA molecules are highly regulated by short sequences or structural motifs, known as regulatory elements. Reversible and dynamic methylation of the mRNA molecule is another regulatory mechanism to influence the metabolism of the molecule (43). Hence, it seems logical that an mRNA molecule that has increased stability can be used as a template for translation for a longer period of time, enhancing the expression of the encoding gene, without a higher amount of cellular mRNA molecules.

Also the amount of functional GPR55 receptors could be influenced by unphysiological oxygen concentrations and the presence of LPI on a different level than the mRNA level. Kargl et al. described in 2012 how specific regulation processes of GPR55 take place on a cellular level. Different to my findings, they could prove that after prolonged LPI stimulation, the GPR55 receptor was down-regulated by internalisation and degradation by GASP-1 (28). Their findings suggest that despite of the influence of LPI, the mRNA expression of GPR55 remains unaffected.

Unfortunately, only 5 different placentas were included in this study. This low case number might have been too small to statistically even out the biological differences that are common in all living tissue. A higher case number might show significant results.

The gestational ages of the placenta tissue I analysed were similar (all between 7+0 and 8+0 weeks); however, the gestational age might still increase the biological differences between the samples, making the analysis of small differences difficult.

Since Matrix metalloproteases and GPR55 play a central role in differentiation and migration one can assume that altered genetic expression of MMPs and GPR55 is associated with altered invasion, migration and tissue regeneration. However, their role in placental development is not yet sufficiently explored. Since many diseases in early pregnancy are associated with impaired trophoblast invasion and vessel transformation, it is suggested that MMPs and GPR55 will be the object of further research.

References

1. Beier H, Beier-Hellwig K, Sterzik K. Die implantationsgerechte Lutealphase des Endometriums.Zum Stand der molekularen und zellbiologischen Forschung. Zentralblatt für Gynäkologie. 2001;123(6):319–27.
2. Oreshkova T, Dimitrov R, Mourdjeva M. A Cross-Talk of Decidual Stromal Cells, Trophoblast, and Immune Cells: A Prerequisite for the Success of Pregnancy. American Journal of Reproductive Immunology. 2012 Nov;68(5):366–73.
3. Rosario GX. Morphological events in the primate endometrium in the presence of a preimplantation embryo, detected by the serum preimplantation factor bioassay. Human Reproduction. 2004 Oct 28;20(1):61–71.
4. Benirschke K, Burton GJ, Baergen RN. Pathology of the Human Placenta. 6th ed. 2012. Springer; 2012. 941 p.
5. Kay H, Nelson DM, Wang Y. The Placenta: From Development to Disease. 1. Auflage. John Wiley & Sons; 2011. 360 p.
6. Morrish DW, Dakour J, Li H. Functional regulation of human trophoblast differentiation. Journal of Reproductive Immunology. 1998 Aug;39(1-2):179–95.
7. Pollheimer J, Knöfler M. The role of the invasive, placental trophoblast in human pregnancy. Wiener Medizinische Wochenschrift. 2012 May;162(9-10):187–90.
8. Harris LK. Review: Trophoblast-Vascular Cell Interactions in Early Pregnancy: How to Remodel a Vessel. Placenta. 2010 Mar;31:S93–S98.
9. Kingdom J, Huppertz B, Seaward G, Kaufmann P. Development of the placental villous tree and its consequences for fetal growth. European Journal of Obstetrics & Gynecology and Reproductive Biology. 2000 Sep;92(1):35–43.
10. Lüllmann-Rauch R, Paulsen F. Taschenlehrbuch Histologie. 4., vollständig überarbeitete Auflage. Thieme, Stuttgart; 2012. 694 p.
11. Sadler TW. Medizinische Embryologie: Die normale menschliche Entwicklung und ihre Fehlbildungen. 11. vollständig überarbeitete. Thieme, Stuttgart; 2008. 530 p.
12. Buerki-Thurnherr T, von M, Wick P. Knocking at the door of the unborn child: engineered nanoparticles at the human placental barrier. Swiss Medical Weekly [Internet]. 2012 Apr 5 [cited 2013 Mar 10]; Available from: http://han.medunigraz.at/han/pubmed/www.smw.ch/content/smw-2012-13559/
13. Jauniaux E, Watson AL, Hempstock J et al. Onset of Maternal Arterial Blood Flow and Placental Oxidative Stress: A Possible Factor in Human Early Pregnancy Failure. 157:2111-22.
14. Hempstock J, Jauniaux E. The contribution of placental oxidative stress to early pregnancy failure. 2003;Volume 34 Issue 12.
15. Murphy G, Nagase H. Progress in matrix metalloproteinase research. Molecular Aspects of Medicine. 2008 Oct;29(5):290–308.
16. Brew K, Nagase H. The tissue inhibitors of metalloproteinases (TIMPs): An ancient family with structural and functional diversity. Biochimica et Biophysica Acta (BBA) - Molecular Cell Research. 2010 Jan;1803(1):55–71.
17. Ii M, Yamamoto H, Adachi Y, Maruyama Y, Shinomura Y. Role of Matrix Metalloproteinase-7 (Matrilysin) in Human Cancer Invasion, Apoptosis, Growth, and Angiogenesis. Experimental Biology and Medicine. 2006 Jan 1;231(1):20–7.
18. Wart HEV, Birkedal-Hansen H. The cysteine switch: a principle of regulation of metalloproteinase activity with potential applicability to the entire matrix metalloproteinase gene family. Proceedings of the National Academy of Sciences of the United States of America. 1990 Jul;87(14):5578.
19. Ali MAM, Fan X, Schulz R. Cardiac sarcomeric proteins: novel intracellular targets of

matrix metalloproteinase-2 in heart disease. Trends Cardiovasc Med. 2011 May;21(4):112–8.
20. Morgunova E, Tuuttila A, Bergmann U, Tryggvason K. Structural insight into the complex formation of latent matrix metalloproteinase 2 with tissue inhibitor of metalloproteinase 2. Proc Natl Acad Sci U S A. 2002 May 28;99(11):7414–9.
21. Cohen M, Meisser A, Bischof P. Metalloproteinases and Human Placental Invasiveness. Placenta. 2006 Aug;27(8):783–93.
22. Nissi R, Talvensaari-Mattila A, Kotila V, Niinimäki M, Järvelä I, Turpeenniemi-Hujanen T. Circulating matrix metalloproteinase MMP-9 and MMP-2/TIMP-2 complex are associated with spontaneous early pregnancy failure. Reproductive Biology and Endocrinology. 2013;11(1):2.
23. Brauer R, Beck IM, Roderfeld M, Roeb E, Sedlacek R. Matrix metalloproteinase-19 inhibits growth of endothelial cells by generating angiostatin-like fragments from plasminogen. BMC Biochem. 2011 Jul 25;12:38.
24. Horn F. Biochemie des Menschen: Das Lehrbuch für das Medizinstudium. 5. Auflage. Thieme, Stuttgart; 2012. 644 p.
25. Baker D, Pryce G, Davies WL, Hiley CR. In silico patent searching reveals a new cannabinoid receptor. Trends Pharmacol Sci. 2006 Jan;27(1):1–4.
26. Balenga NAB, Henstridge CM, Kargl J, Waldhoer M. Pharmacology, Signaling and Physiological Relevance of the G Protein-coupled Receptor 55. Advances in Pharmacology [Internet]. Elsevier; 2011 [cited 2013 Mar 18]. p. 251–77. Available from: http://han.medunigraz.at/han/pubmed/www.sciencedirect.com/science/article/pii/B978012385952500004X
27. Henstridge CM, Balenga NAB, Kargl J, Andradas C, Brown AJ, Irving A, et al. Minireview: Recent Developments in the Physiology and Pathology of the Lysophosphatidylinositol-Sensitive Receptor GPR55. Molecular Endocrinology. 2011 Sep 29;25(11):1835–48.
28. Kargl J, Balenga N, Platzer W, Martini L, Whistler J, Waldhoer M. The GPCR-associated sorting protein 1 regulates ligand-induced down-regulation of GPR55. British Journal of Pharmacology. 2012 Apr;165(8):2611–9.
29. Fonseca BM, Teixeira NA, Almada M, Taylor AH, Konje JC, Correia-da-Silva G. Modulation of the novel cannabinoid receptor - GPR55 - during rat fetoplacental development. Placenta. 2011 Jun;32(6):462–9.
30. Balenga NAB, Aflaki E, Kargl J, Platzer W, Schröder R, Blättermann S, et al. GPR55 regulates cannabinoid 2 receptor-mediated responses in human neutrophils. Cell Research. 2011 Apr 5;21(10):1452–69.
31. Whyte LS, Ryberg E, Sims NA, Ridge SA, Mackie K, Greasley PJ, et al. The putative cannabinoid receptor GPR55 affects osteoclast function in vitro and bone mass in vivo. Proceedings of the National Academy of Sciences. 2009 Sep 3;106(38):16511–6.
32. Andradas C, Caffarel MM, Pérez-Gómez E, Salazar M, Lorente M, Velasco G, et al. The orphan G protein-coupled receptor GPR55 promotes cancer cell proliferation via ERK. Oncogene. 2010 Sep 6;30(2):245–52.
33. Ford LA, Roelofs AJ, Anavi-Goffer S, Mowat L, Simpson DG, Irving AJ, et al. A role for L-α-lysophosphatidylinositol and GPR55 in the modulation of migration, orientation and polarization of human breast cancer cells. British Journal of Pharmacology. 2010 Mar 11;160(3):762–71.
34. Piñeiro R, Falasca M. Lysophosphatidylinositol signalling: New wine from an old bottle. Biochimica et Biophysica Acta (BBA) - Molecular and Cell Biology of Lipids. 2012 Apr;1821(4):694–705.
35. Van Corven EJ, Groenink A, Jalink K, Eichholtz T, Moolenaar WH. Lysophosphatidate-induced cell proliferation: Identification and dissection of signaling pathways mediated by G proteins. Cell. 1989 Oct;59(1):45–54.
36. Falasca M, Corda D. Elevated levels and mitogenic activity of lysophosphatidylinositol in k-ras-transformed epithelial cells. European Journal of Biochemistry. 1994 Apr;221(1):383–9.
37. Oka S, Nakajima K, Yamashita A, Kishimoto S, Sugiura T. Identification of GPR55 as a lysophosphatidylinositol receptor. Biochemical and Biophysical Research Communications. 2007

Nov;362(4):928–34.
38. Mülhardt C. ˜Derœ Experimentator Molekularbiologie/Genomics. Berlin, Heidelberg: Imprint: Springer Spektrum; 2013.
39. Heid CA, Stevens J, Livak KJ, Williams PM. Real time quantitative PCR. Genome Res. 1996 Oct 1;6(10):986–94.
40. S.S. Shapiro; M.B: Wilk. An Analysis of Variance Test for Normality. (Vol. 52, No.3/4. (Dec.,1965),):pp. 591–611.
41. Clark I, Swingler T, Sampieri C, Edwards D. The regulation of matrix metalloproteinases and their inhibitors. The International Journal of Biochemistry & Cell Biology. 2008 Jun;40(6-7):1362–78.
42. Holtkamp S, Kreiter S, Selmi A, Simon P, Koslowski M, Huber C, et al. Modification of antigen-encoding RNA increases stability, translational efficacy, and T-cell stimulatory capacity of dendritic cells. Blood. 2006 Dec 15;108(13):4009–17.
43. Wang X, Lu Z, Gomez A, Hon GC, Yue Y, Han D, et al. N6-methyladenosine-dependent regulation of messenger RNA stability. Nature. 2013 Nov 27;505(7481):117–20.